

**Spectral phase correction of femtosecond
pulses using a deformable mirror.**

Laboratoire d'Optique Appliquée
ENSTA, Ecole Polytechnique, CNRS

by
Veronica Wänman

Master's Thesis
Lund Reports on Atomic Physics, LRAP-258,
Lund, June 2000

Abstract

A new method to correct the residual spectral phase has been implemented in a 40fs, 1kHz chirped-pulse-amplification laser at Laboratoire d'Optique Appliquée at ENSTA-Ecole Polytechnique-CNRS, in Paris. The spectral phase of the output pulse was made flatter by introducing an opposite spectral phase in the laser chain. The opposite spectral phase was created with a deformable mirror placed directly in the Fourier plane of the stretcher, hence no extra losses were added. The spectral phase was minimised with a feedback loop including the deformable mirror, a SPIDER, that measured the spectral phase, and an algorithm, which calculated the new shape of the mirror. The spectral phase was reduced from 2 rad to 0.4 rad peak-to-valley on a 45 nm spectral range. The contrast of the output pulse was also greatly improved.

Table of contents

1. Introduction	4
1.1. A historical perspective	4
1.2. Femtosecond laser	4
1.3. Temporal profile	4
1.4. Purpose of this master thesis	5
2. Theory	7
2.1. The laser chain	7
2.2. Dispersion and the spectral phase	7
2.3. Oscillator	9
2.3.1. Criteria for oscillation	9
2.3.2. Mode-Locking	10
2.3.3. Pulse duration	11
2.3.4. Dispersion compensation	11
2.4. Compressor	12
2.4.2. Spectral cut	13
2.5. Stretcher	13
2.5.2 Spherical aberrations	14
2.6 Regenerative Amplifier	15
2.6.1. Free-running mode	15
2.6.2. Amplification	15
2.6.3. Gain narrowing	16
2.6.4. Phase distortion	16
2.7. Minimisation of the spectral phase in CPA system	16
3. Numerical optimisation	18
4. Experimental set-up	19
4.1. Laser chain	19
4.2. Oscillator	20
4.2.1. Technical information	20
4.2.2. Pulse duration	20
4.3. Regenerative Amplifier	21
4.3.1. Set-up	21
4.3.2. Pockels cell	21
4.3.3. Amplification process	22
4.4. Compressor	23
4.5. Stretcher	24
4.5.1. Stretcher model	24
4.5.2. Grating frame	25
4.5.3. Feedback loop	26
4.5.3.1. Deformable mirror	27
4.5.3.2. Control algorithm	27
4.5.3.3. Feedback loop	28
4.5.3.3. Capacity of the deformable mirror	28

4.6. SPIDER	29
4.6.1. Spectral shearing interferometry	29
4.6.2. SPIDER set-up	30
5. Results	31
5.1. Regenerative Amplifier	31
5.1.2. Objective	31
5.2.2. Results	31
5.2.3. Free-running mode	31
5.2.4. Amplification	32
5.3. Deformable mirror	32
5.3.1. Objective	32
5.3.3. Results	33
5.3.3.1 Spectral phase	33
5.3.3.2. Contrast and duration	34
6. Conclusion and Prospects	35
Acknowledgements	36
References	37
Appendix : Alignment of the stretcher	38

1. Introduction

1.1. A historical perspective

The first laser was built in 1960 by T.H. Maiman. It was a continuous laser with a ruby crystal as the gain medium. Almost forty years later, in 1999, Professor A.H. Zewail was awarded the Noble Prize in chemistry for an application of femtosecond lasers ($1\text{fs} = 10^{-15}\text{s}$). He had developed a technique to measure chemical reactions in real time based on femtosecond spectroscopy. This would not have been possible without the development of femtosecond lasers.

1.2. Femtosecond laser

Researchers strive to develop shorter pulses, more energetic pulses and higher repetition rates. The most important techniques that have resulted in amplified femtosecond pulsed lasers are presented in the paragraph below.

The production of short pulses began with the Q-switching technique and then the mode-locking technique, both developed in the early 1970's. This led to pulses as short as 1ps, ($1\text{ps} = 10^{-12}\text{s}$). In 1985, the Chirped Pulse Amplification technique was developed. Prior to this technique it was not possible to amplify ultra short pulses because they reached intensities that produced non-linear effects and finally destroyed the optical material in the amplifier. In a CPA laser, the pulse is stretched in duration before amplification in a stretcher. The intensity is therefore reduced before the pulse enters the amplifier. After amplification the pulse is re-compressed to its original duration in a compressor. The CPA technique allows hence amplification of very short pulses. Another advantage with the CPA technique is that undesired non-linear effects are prevented in the amplifying medium.

The shortest pulses today are produced with the mode-locking technique, which uses the size of the bandwidth of the gain medium to produce ultra-short pulses. A good crystal is the Ti:sapphire crystal. The Ti:sapphire crystal has a very large bandwidth, which corresponds to a minimum duration¹ of 4.5fs in a mode-locked laser, ref. [1]. Another advantage with the Ti:sapphire crystal is its capability to store a lot of energy. The combination of large bandwidth and large storage of energy has made the Ti:sapphire the most common gain medium for high peak power femtosecond lasers.

1.3. Temporal profile

The development of shorter and shorter pulses has led to new problems. Today it is not only the duration and the energy of the laser pulse, but also the contrast² that is important. The temporal shape of the laser pulse is critical in the studies of the interaction of light and matter. The peak pulse can be surrounded by wings consisting of one or more pre and post pulses³. Consequently these wings decrease the energy in the main pulse peak. Further if the pre-pulses are large enough they can cause undesired plasma production. The plasma then absorbs a large

¹ This is the minimum theoretical duration calculated with the time-bandwidth product, see section 2.4.3.

² The ratio between the peak pulse and its wings is called the contrast.

³ Pre and post pulse appear before, $t < 0$, the main pulse peak, $t = 0$, and after, $t > 0$, respectively.

part of the pulse's peak energy that was intended for the target. In the following paragraph the source of this contrast problem is explained and different solutions are presented.

The temporal shape of the laser pulse is subject to several modifications during its propagation through the laser chain. These modifications are due to dispersion effects due to passage through optical mediums and to aberrations introduced by optical systems in the laser chain. Dispersion and aberrations introduce a phase, which is frequency⁴ dependent. This phase is called the spectral phase, $\phi(\omega)$. The spectral phase deforms the temporal profile of the laser pulse. There are two different approaches to solve this problem :

1. Design laser chain components with a minimum amount of the spectral phase introduced.
2. Introduce an opposite spectral phase that compensates for the spectral phase caused by the laser chain.

The common approach to the first alternative is to develop an aberration free stretcher design. In such a configuration the dispersion effects introduced can be compensated for in the compressor. However since the stretcher includes an optical system it is not an easy task. An aberration free stretcher design was constructed by G.Chériaux et al., ref. [2] in 1996, in which the spectral phase is flat and the pulse duration was only limited by the size of the components. The drawback to this system is the precise alignment required.

Several methods have been developed based on the second idea, such as introduction of a spectral phase that compensates that of the laser chain. In 1997, P. Tournois presented an acousto-optic programmable dispersive filter, ref. [3], for spectral phase compensation. An acoustic signal generated a pre-chirped optical signal by interaction in an anisotropic birefringent medium. Compensation for linear chirp was achieved. A more popular approach is to place a liquid crystal filter, called a spatial light modulator, in a zero-dispersion line. The laser pulse is transmitted through the crystal liquid filter and the spectral phase is reduced by varying the refractive index for different wavelengths⁵. This method can achieve a very flat phase, 0.3 rad peak-to-valley, ref. [4]. However, this filter is used for transmission and adds therefore an extra energy loss in the laser chain.

1.4. Purpose of this master thesis

This master thesis was carried out at Laboratoire d'Optique Appliquée, which is a part of Ecole Nationale Supérieure de Techniques Avancées, Ecole Polytechnique and CNRS, and situated in Paris.

The purpose of this master thesis was to implement a new method for spectral phase reduction. The method is a combination of the two different approaches presented in the previous section. A stretcher design is chosen that limits the introduced aberrations to only spherical aberrations. Further, a new approach is taken to the second method, introduction of a correcting spectral phase. Instead of placing a phase modulating filter in a zero-dispersion line, a deformable mirror is placed directly in the stretcher. The mirror is then shaped such that it introduces a

⁴ Since the phase is frequency dependent it is also wavelength dependent.

⁵ In a zero dispersion line the different wavelengths are spatially distributed on a line. Hence by spatially varying the refractive index of the liquid crystal one varies the refractive index for different wavelength components. A spectral phase is introduced.

spectral phase opposite to the one introduced by the laser chain. The shape of the mirror is controlled with a feedback loop including a SPIDER, which measures⁶ the spectral phase, and an algorithm. This method allows an easy alternative to correcting the total spectral phase introduced in a CPA system. Compared to the transmitting filter placed in a zero-dispersion line, this solution does not add any extra losses since it is a reflective material placed directly in the stretcher.

To be able to verify this method, a CPA laser had to be completed. At the start of this project only the oscillator existed, during the project a stretcher, compressor and regenerative amplifier have been built.

⁶ The SPIDER is an interferometric method with which one obtains the spectral phase of the laser pulse.

2. Theory

2.1. The laser chain

This section is intended to give the reader a fast overview of the femtosecond laser chain built and used during this master thesis. The components' functions are briefly explained and their effect on the laser pulse demonstrated with an example.

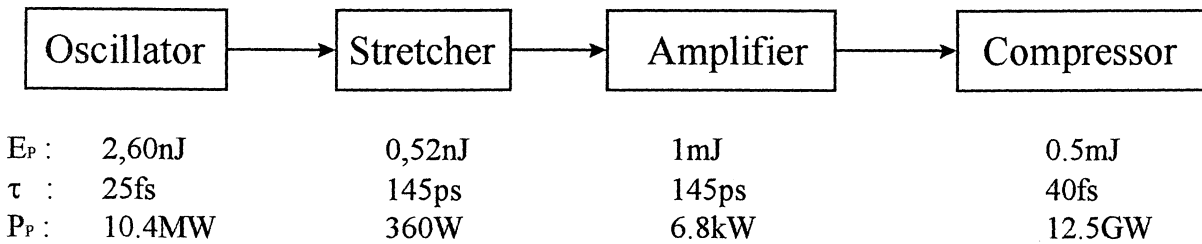


Fig 1. The chirped pules amplified laser consist of an oscillator, which creates the pulse, a stretcher that increase the duration of the pulse, before amplification in the amplifier, finally the pulse is compressed in the compressor.

Notations:

E_P : Pulse energy [J]

τ : Duration [s]

P_P : Peak power [W]

The oscillator

The pulse is generated in the oscillator. The oscillator characteristics set the pulse's duration, the spectral width and the repetition rate of the output beam.

The Stretcher

The stretcher increases the duration of the pulse, without reducing the bandwidth, and therefore decreases the pulse intensity. The stretcher is needed to avoid non-linear effects and damage to the optical materials in the amplifier.

The Amplifier

The amplifier increases the pulse energy, but reduces the bandwidth due to gain narrowing. The amplifier model can be neither a Regenerative Amplifier, a Multi-pass amplifier or a combination of both. The method chosen depends on the desired energy level.

The Compressor

The compressor is the final component in our laser chain. Its task is to compress the pulse to its original duration. However this is not possible because of dispersion, gain narrowing and other limiting effects in the laser chain.

2.2. Dispersion and the spectral phase

The laser pulse temporal and spectral shape is modified during its propagation through the laser chain. Aberration and transmission through optical medium causes dispersion, which introduces a spectral phase. Further, the spectral width is reduced due to spectral cut and gain narrowing. The basic theory behind these effects is discussed in this chapter.

Dispersion is introduced when a chromatic wave passes an optical medium because the refractive index is wavelength dependent. Therefore, dispersion introduces a spectral phase since the different segments of the pulse are shifted in time compared to the central frequency. The effect of dispersion depends on the amplitude but also on the bandwidth of the laser pulse.

For example, the dispersion effects introduced in the stretcher are important for femtosecond¹ pulses but negligible for nanosecond pulses, ref. [5]. The relationship between the spectral phase and the frequency can be developed in a Taylor series, ref. [5] :

$$\phi(\omega) = \phi_0 + \phi^{(1)}\Omega + \frac{1}{2}\phi^{(2)}\Omega^2 + \frac{1}{6}\phi^{(3)}\Omega^3 + \frac{1}{24}\phi^{(4)}\Omega^4 + \dots \quad (1)$$

$$\text{where : } \Omega = \omega - \omega_0, \phi^{(n)} = \frac{d^n \phi}{d\omega^n}, \text{ with } \omega \text{ set to } \omega_0$$

The first term, ϕ_0 , is a constant and can be neglected. The second term, $\phi^{(1)}\Omega$, is the first order of dispersion. The third term, $1/2\phi^{(2)}\Omega^2$, is called the group velocity dispersion or the chirp. The fourth term, $1/6\phi^{(3)}\Omega^3$, is called the third order dispersion and so forth. The temporal change that the spectral phase introduces is more easily understood if studying the propagation delay. The propagation delay $T(\omega)$ is defined as, ref. [5] :

$$\begin{aligned} T(\omega) &= \frac{d\phi(\omega)}{d\omega} = \\ &= \phi^{(1)} + \phi^{(2)}\Omega + \frac{1}{2}\phi^{(3)}\Omega^2 + \frac{1}{6}\phi^{(4)}\Omega^3 + \dots \quad (2) \\ &= T_1(\Omega) + T_2(\Omega) + T_3(\Omega) + T_4(\Omega) + \dots \end{aligned}$$

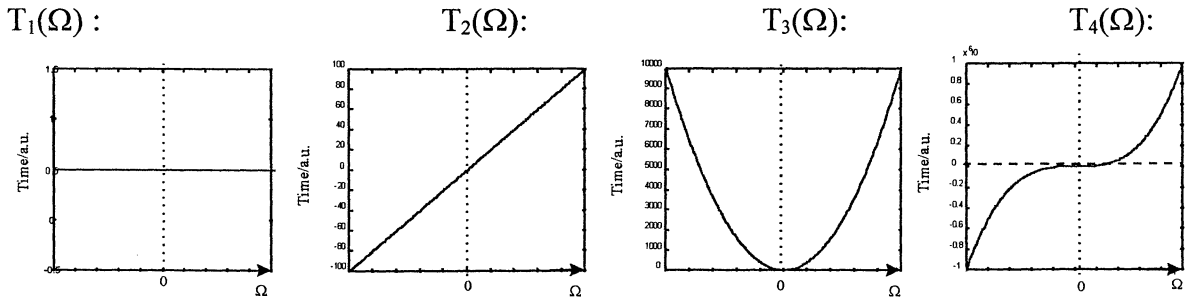


Fig 2. The shape of the different orders of the propagation delay T as a function of frequency. The central frequency is marked with a vertical dashed line. The central frequency ω_0 corresponds to 800nm, which is usually the central wavelength in Ti:sapphire femto second lasers.

- T_1 : The first order dispersion causes a delay of propagation that is constant, see fig. 2. All frequencies are delayed with the same time t .
- T_2 : The second order dispersion introduces a linear delay as a function of the frequency, thereof the name linear chirp . The pulse duration is increased with the short frequencies ahead and long frequencies behind, positive chirp or vice versa, negative chirp.
- T_3 : The third order dispersion causes an asymmetric delay of the pulse. The frequencies close to the central frequency are less delayed than the ones at the end of the spectre, see fig. 2. Parasite pulses appears before or after the main pulse depending on the sign of $\phi^{(3)}$ and the pulse shape is no longer Gaussian.
- T_4 : The fourth order dispersion introduces a symmetrical pedestal around the main pulse. The duration of the pulse is also slightly increased.

¹ Theoretical bandwidths for a pulse of length 40fs with central wavelength at 800nm is 25nm if considered of Gaussian shape and transform limited.

2.3. Oscillator

The oscillator is the first part in the laser chain and the source of the laser pulse. Hence the oscillator parameters set the characteristics of the laser pulse. The duration of the pulse depends on the bandwidth of the gain medium and on the GVD compensation in the cavity. Further the repetition rate is set by the cavity length. Femtosecond pulses are generated with a technique called mode-locking. This technique and the criteria for oscillation are presented in this section.

2.3.1. Criteria for oscillation

The frequencies of the longitudinal modes in a laser cavity have to fulfil two criteria. The longitudinal modes have to be resonant frequencies of the cavity. This means that their frequencies have to be:

$$\nu_k = \frac{c}{2L} k, \quad (3)$$

Where k is an integer, c the velocity of light and L the length of the cavity.

Equation (3) shows that the oscillating modes are equally separated in frequency, see also figure a. Further the frequencies have to be within the gain width of the active medium otherwise the cavity losses prevent the mode from oscillating. Hence only the modes that fulfil both criteria can exist in the cavity, see fig. 3c.

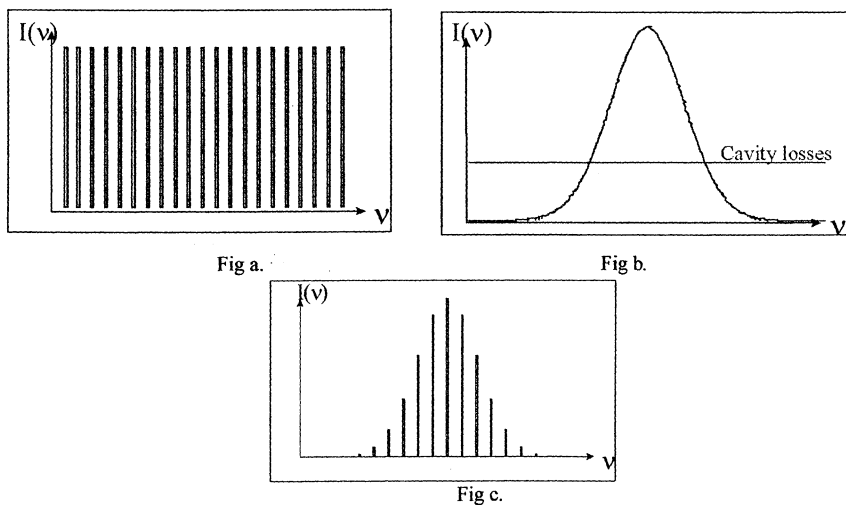


Fig.3 a. The longitudinal modes that fulfil equation 3. The modes are separated by $\Delta\nu=c/2L$ in frequency., b. the gain of the active medium and the cavity losses, c. the modes that are amplified in the cavity.

2.3.2. Mode-Locking

The mode-locking technique is based on constructive interference between the oscillating modes in the laser cavity. The result is a short pulse that travels back and forth in the cavity. The word mode-lock comes from the fact that the phases of the oscillating modes are locked in phase.

Initially the modes oscillate independent of each other with random phases. The laser is in continuous mode. The output beam is a periodic noise, whose intensity I is the summation of all the oscillating modes. However, with mode-locking techniques the modes are set in phase and constructive interference produces one short pulse whose intensity is $n^2 I'$, where n is the number of modes, ref. [1].

The oscillator in Salle Turquoise uses a passive mode-locking method, the Kerr lens. The optical Kerr effect occurs when the beam intensity is so high that the refractive index becomes intensity dependent. The first order Taylor expansion of $n(I)$ is, ref. [6]:

$$n(I) = n_0 + n_2 I \quad (4)$$

The value of n_2 depend on the material, but is always positive.

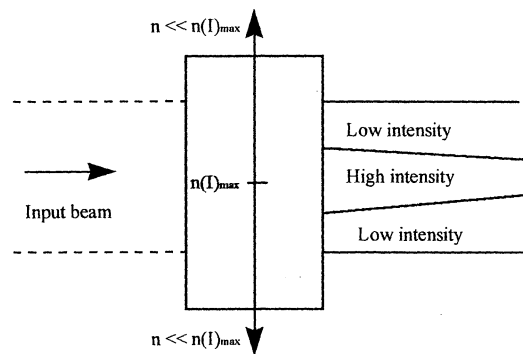


Fig 4. The Kerr lens : The Ti :sapphire crystal behaves as a convergent crystal for high intensity beams. The refractive index increases with intensity, see equation 2. The spatial profile of the input beam is Gaussian and hence the part closest to the optic axis experience a higher refractive index than the boarder of the pulse, see equation 4. The result is called self focusing. However this effect is only valid if the beam has a sufficient intensity, compare the paths of the High and Low intensity beam above.

The spatial beam shape in the cavity is Gaussian. Light on the optic axis experiences therefore a higher refractive index than light further from the centre. At high intensities the Ti :sapphire crystal becomes a convergent lens and the beam is self-focused, see fig. 4. Next passage the intensity is higher, the self focus effect greater and so forth. The modes oscillating in phase have therefore an advantage since their total intensity is greater than the modes interfering without any phase connection. However this profitable process does not start by itself.² It has to be initiated by perturbation. The perturbation used in Salle Turquoise is a vibrating mirror, which changes the length of the cavity. The cavity is more stable with Kerr lens than without. It is sufficient to introduce one short distance change, one vibration pulse, and the cavity becomes and stays mode-locked. The mode-locking is maintained without any external signal, and so it is called passive mode-locking.

² The intensities created during the continuous mode are too small to make the gain medium behave as a Kerr lens.

2.3.3. Pulse duration

The pulse duration is limited by the bandwidth of the gain medium. The relationship between the duration, $\Delta\tau$, and the pulse bandwidth, $\Delta\nu$ is called the time-bandwidth product:

$$\Delta\tau \cdot \Delta\nu \geq K, \quad (5)$$

K is a constant that depends on the shape of the pulse, for Gaussian it is 0.441. When equality is achieved the pulse is transform limited. The gain bandwidth of Ti:sapphire is 200nm. For a Gaussian shaped pulse the minimum duration is 4.5fs, ref. [1].

2.3.4. Dispersion compensation

The Ti:sapphire crystal is, like most optical media, a source of positive group velocity dispersion. In order to minimise the pulse duration, the positive GVD has to be compensated within the cavity itself. A prism pair with negative GVD used at double passage is commonly used in femtosecond cavities, see figure below:

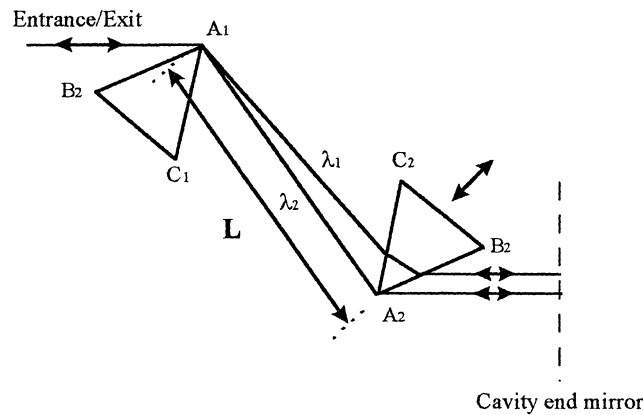


Fig 5. A prism pair with negative GVD. The shorter wavelengths, λ_1 , travel a farther length inside the prisms and is therefore delayed in time relative the longer wavelength λ_2 . The length L determines the amount of GVD and is optimised so that it compensates for the positive GVD introduced in the gain medium. The bandwidth of the mode-locked pulse can be varied by changing the position of the second prism, see arrow.

Long wavelengths are deviated more than the short wavelengths by the first prism, compare pathways for the two wavelengths λ_1 and λ_2 in the figure, $\lambda_1 < \lambda_2$. Notice that the exit plane A_1C_1 of the first prism is parallel to the entrance plane of the second prism, A_2C_2 . The short wavelength will hence travel a longer distance within the second prism than the longer ones. Negative GVD is introduced. The beam is parallel after the second prism. A mirror, usually the cavity end mirror, is placed after the second prism. After double passage through the prism pair the pulse has been compressed in time. The distance between the two prisms is chosen so that it compensates for the positive group velocity dispersion introduced in the Ti:sapphire crystal.

There are several advantages with this prism configuration. Losses are minimised because all prism planes are at Brewster angle relative to the beam path. Further the size of the bandwidth can be easily adjusted by changing the amount of glass the pulse beam traverses in the second beam, see arrow in fig. 5. The prism pair introduces negative dispersion, which compensates the positive dispersion introduced by material dispersion in the Ti:sapphire crystal. Consequently by changing the amount of negative dispersion the total dispersion in the cavity

can be increased or decreased³. If the total dispersion is decreased there are more modes that can oscillate in phase and hence the bandwidth of the pulse beam becomes larger and vice versa.

2.4. Compressor

The compressor is an optical system with negative chirp, long wavelengths travel a longer distance than the short ones.⁴ A pulse with positive chirp is compressed in time after passage through the compressor. In 1969 E.B. Treacy, ref. [7], presented the theory of the compressor model used in our system. Today it is a widely used design in femtosecond laser systems.

The compressor consists of two parallel gratings, G_1 and G_2 and a roof prism, see figure. The beam has an incidence angle θ_i and is diffracted at an angle θ_d by the first grating, G_1 , such that the central wavelength propagates along the optical axis. The compressor operates at diffraction order -1 because the efficiency of the gratings are greatest at this order. The second grating is positioned parallel to the first at a distance L_c , the compressor length. After diffraction by the second grating the pulse is spatially chirped. In order to maintain the beam size the pulse passes the compressor twice in two parallel vertical planes. This is obtained by placing two mirrors at 90 degrees, after the second grating.

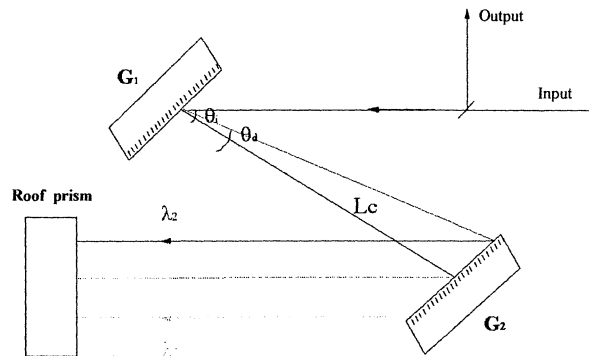


Fig 6. The compressor : The input pulse is incident on the first grating G_1 with an angle θ_i to the normal. The spectral components of the pulse are then refracted at different angles, θ_d , determined by the law of diffraction. The two gratings are parallel so the incidence angle is conserved through the system. After diffraction at the second grating, G_2 , the pulse beam is parallel with its spectral components in line, see the paths of λ_1 and λ_2 . The beam is reflected by the roof prism and passes through the compressor a second time in a parallel vertical plane. After the double passage the two wavelengths have travelled different lengths, $L(\lambda_2) > L(\lambda_1)$, and negative chirp has been introduced. The amount of negative chirp introduced depends on the compressor length L_c and on the incidence angle θ_i .

The compression of a positively chirped pulse is illustrated with two spectral pulse components λ_1 and λ_2 , where $\lambda_1 > \lambda_2$. The two components enter the compressor at different times, $t_{in1} > t_{in2}$, since the pulse has a positive chirp. In the compressor the two components follow two different paths, see λ_1 and λ_2 , determined by the law of diffraction. The law of diffraction is :

$$\sin \theta_i + \sin \theta_d = \frac{n\lambda}{d} \quad (6)$$

³ The larger amount of glass traversed the greater difference in optical distance between the different wavelengths. Therefore by increasing this optical distance a larger negative dispersion is introduced.

⁴ In frequency terms : The pulse components at low frequency travel a longer distance than the high frequency pulse components.

Where θ_i is the incidence angle, θ_d is the diffraction angle,
 n the order of diffraction, λ the wavelength and d the diffraction spacing.

The compressor length and the incidence angle are chosen such that the two spectral components exit the compressor at the same time, $t_{out1}=t_{out2}$. The pulse has been compressed in time.

2.4.2. Spectral cut

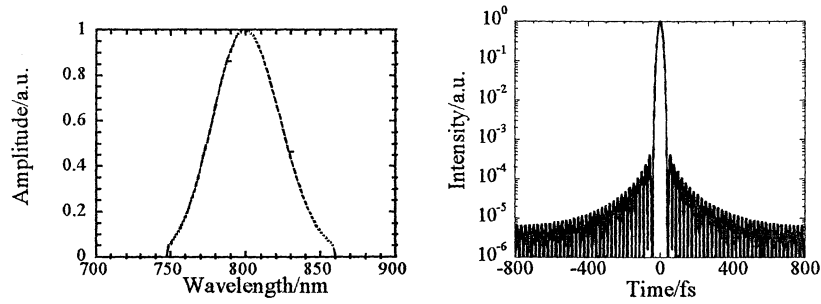


Fig 7. a. A spectrally cut Gaussian shaped pulse, observe the sharp edges on both sides.
 b. The temporal shape of the spectrum in a. The spectral cut causes the symmetrical pedestal around the peak pulse.

The finite element size of the components in the stretcher and the compressor limits the spectral range of the laser pulse. This effect is appropriately called the spectral cut, since the spectrum is abruptly limited at its edges. The temporal shape of a spectrally cut pulse is calculated with the Fourier Transform of the limited spectrum. The response function of the spectral cut is a rectangular function, see ref. [5]. This corresponds to a sinus cardinal⁵ - in the time domain, see fig. 7b. The spectral cut causes a symmetrical pedestal, which decreases the contrast. The size of the spectral cut has therefore to be taken into consideration when choosing the elements in the stretcher and compressor.

2.5. Stretcher

In 1987 Martinez, ref. [8], developed a stretcher based on Treacy's compressor model presented in the previous section. This stretcher is a compressor with positive group velocity dispersion, which is obtained by an effective negative compressor length, $L_S = -L_C$. The ideal stretcher introduces therefore a spectral phase exactly opposite to that of the compressor.

⁵ The Fourier transform of a Gaussian function multiplied by a rectangular function is a sinus cardinal, ref. [5].

Two refractive gratings are placed anti-parallel to each other with a one-to-one telescope, $G=-1$, placed in-between. An effective negative distance is achieved if the image of the first grating, G'_1 , is behind the second grating, G_2 , and parallel to the latter, see fig. 8.

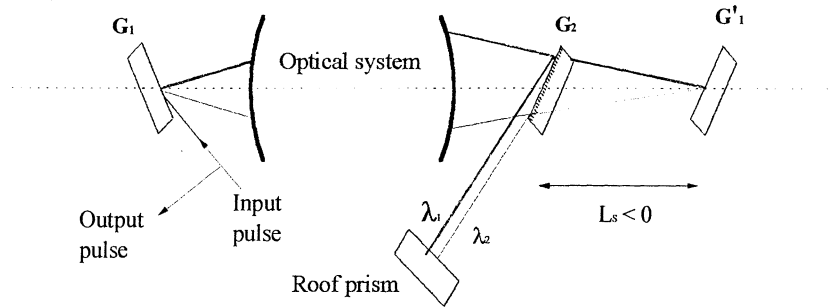


Fig 8. The stretcher :The basic procedure is the same as for the compressor. However after the diffraction by the first grating, G_1 , the pulse passes a one-to-one telescope that inverts the image, $G=-1$. The incident beam on the second grating G_2 has therefore the characteristics of a pulse diffracted by G'_1 , the inverted image of G_1 . The distance between the image G'_1 and the second grating G_2 is negative, $L_s > 0$. After diffraction by the second grating the beam is parallel and the position of the wavelengths reversed compared to after one passage through the compressor. The beam is reflected by the roof prism and passes through the stretcher a second time in a parallel vertical plane, like in the compressor. In the stretcher a positive chirp is introduced the shorter wavelengths have travelled a longer distance than the longer ones, $L(\lambda_1) > L(\lambda_2)$. The amount of positive chirp introduced depends on the length of the stretcher, L_s and the incidence angle θ .

The one-to-one telescope can be a set of converging lenses or spherical mirrors. Both alternatives introduce aberrations, which limit the duration of the pulse. Converging lenses cause spherical and chromatic⁶ aberration, the latter can be partly compensated for by using achromatic lenses. Spherical mirrors do not introduce chromatic aberrations, since it is a reflecting material. However the problem with spherical aberration remains. Spherical aberrations introduce a spectral phase of the fourth order, ref. [5]. The stretcher is not compatible with the compressor and the minimum pulse duration is limited.

2.5.2 Spherical aberrations

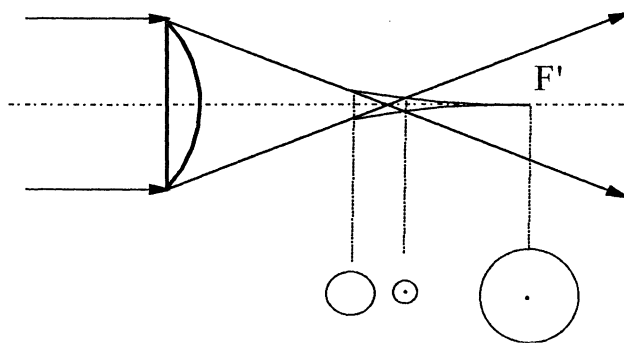


Fig 8. A parallel beam is incident on a convergent lens. The non-paraxial rays converge faster than the paraxial rays. All rays do not have the same focal point. The three rings correspond to the image seen at the different planes.

The concave mirror in the stretcher introduces higher order dispersion terms due to spherical aberration. Parts of the diffracted pulse, incident on the spherical mirror, are so far from the optic axis that it cannot be considered paraxial. Non-paraxial rays converge earlier than paraxial rays, see fig 8. This is called spherical aberration.

⁶ Chromatic aberration is caused by the focal points wavelength dependence.

All frequencies are not focused on the Fourier plane of the mirror. Consequently the incidence angle is not conserved through the stretcher and fourth order dispersion is introduced, ref. [5]. Further, the diffracted beam's components' distance from the optical axis depends on frequency, with the central frequency on the axis. The function is not linear, but determined by the law of refraction. This results in dispersion of order greater than the fourth, ref. [5]. However in our laser chain the higher order terms are negligible.

2.6 Regenerative Amplifier

The regenerative amplifier is a laser cavity without an output coupling mirror. Instead the entrance and exit are externally controlled by, for example a Pockels cell and a polarizer. The regenerative amplifier operates either at free-running mode or with injection and extraction.

2.6.1. Free-running mode

The regenerative amplifier in our laser system is a three mirror cavity with a gain medium and a shutter. The shutter controls the entrance and exit of the cavity. When the external control is turned off, no entrance or exit is possible, and the cavity operates at free-running mode. Laser effect is achieved due to amplified spontaneous emission, ASE. The gain medium is pumped with a pulsed laser at a time interval much greater than the decay time of the gain medium. Hence the cavity operates in pulsed mode. The free-running mode is primarily used to align and optimise the cavity.

2.6.2. Amplification

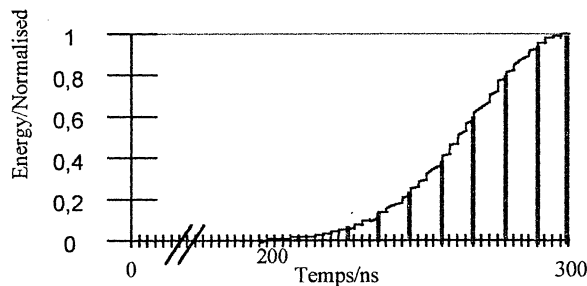


Fig 9. The amplification of the laser pulse after each passage through the gain medium. The pulse is ejected after 300ns when it has reached the maximum energy.

The purpose of the regenerative amplifier is to amplify low energetic pulses, nJ, to the mJ level. The shutter is then activated such that the pulse enters the exit at the right moment for maximum amplification. The synchronisation between the pump beam and the entrance of the pulse is crucial. The gain medium is pumped while the shutter prevents laser effect, ASE, until the inverted population has reached its maximum value⁷. The time for entrance is timed such that the pumped energy is not lost in fluorescence. The incoming beam has much higher energy than ASE and becomes the favoured mode. The injected pulse is therefore amplified each passage through the gain medium until the inverted population has decreased to the level at which the cavity losses are greater than the gain in the crystal. The pulse will then lose more energy than it gains per cavity round-trip. Just before this happens the pulse is extracted from the cavity. The rest of the energy in the gain medium is lost through fluorescence. The

repetition rate is chosen such that it is much longer than the crystal's decay time, hence the inverted population is zero when the gain medium is pumped the next time.

2.6.3. Gain narrowing

The bandwidth of the laser pulse decreases after each passage through the gain medium in the regenerative amplifier. The effective gain of the Ti :sapphire is wavelength dependent and pulses close to 800nm are favoured. The pulse's central wavelengths are therefore more amplified than the wavelengths on the edges of the spectrum. The difference in amplitude between the central part and the edges of the pulse increase after each passage through the gain medium. This phenomenon is called gain narrowing. Gain narrowing becomes less important when saturation effects occur in the gain medium, which sets a limit to how much the bandwidth is reduced. The consequence of gain narrowing is an increase in pulse duration, which makes it impossible to obtain the original pulse duration after compression in the compressor.

2.6.4. Phase distortion

The pulse is transmitted through several optical media during its amplification in the regenerative amplifier. These media, Ti :sapphire crystal, KDP crystal, polarizer, are all sources of dispersion, since their refractive indexes are wavelength dependent. The spectral phase introduced due to transmission through an optical medium can be expressed as, ref.[5]:

$$\phi(\omega) = \frac{2\pi}{c}n(\omega)L, \quad (7)$$

Where $n(\omega)$ is the refractive index of the optical medium, L is the length of the medium and c the velocity of light.

The different orders of dispersion are then obtained by derivation of equation (7), ref.[5] The sign of the second and third order dispersion is positive, while the sign of the fourth order dispersion is material dependent, ref.[5].

Equation (7) shows that the phase distortion introduced is dependent on the amount of material traversed, L . It is therefore very important to minimise the number of round-trips in the regenerative amplifier. The phase distortion that remains after optimisation is corrected for in the stretcher and the compressor as presented in the following section.

2.7. Minimisation of the spectral phase in CPA system

The stretcher, the compressor and the regenerative amplifier are all sources of dispersion. The spectral phase introduced in the compressor and the stretcher are of opposite sign if the stretcher is aberration free. The spectral phase can hence be reduced if the compressor and stretcher system is optimised.

The stretcher and the compressor have each three degrees of freedom. The spectral phase in the CPA chain is optimised by changing the parameters of the compressor without adjusting the stretcher. The three degrees of freedom are :

- the compressor length L [mm]
- the incidence angle θ [°]
- the diffraction grating spacing d [grooves/mm]

These correct for second, third and fourth order dispersion respectively. However in practice L, θ and d are optimised together in order to minimise the total spectral phase. For example, fourth order dispersion can be partly compensated for by introduction of an opposed second order dispersion, ref.[2], see fig 10b. However the stretcher design used in this thesis work allows for correction of higher order dispersion terms by themselves. The deformable mirror, part of the stretcher, is shaped such that it introduces a spectral phase opposite to the one produced by the laser chain itself. This will be further explained in the next chapter.

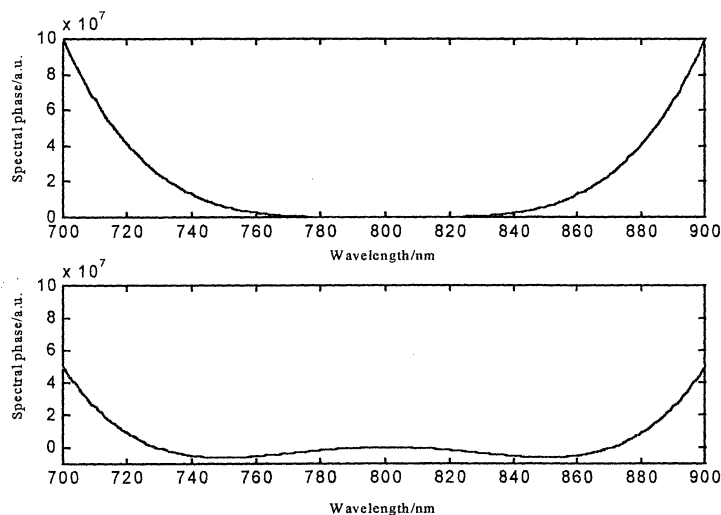


Fig 10. a. The fourth order of dispersion, $\phi(4)$, as a function of wavelength.
 b. Fourth order of dispersion compensated with a negative second order of dispersion.
 Notice the difference in spectral range over which the spectral phase is flat.

Finally the minimisation process of the spectral phase can be divided into two stages. First a theoretical optimisation that is done before installation of the components in the laser. Once the components are installed the grating spacing, d , remains fix⁸. The remaining spectral phase is therefore minimised by optimisation of the compressor length and the incidence angle⁹.

⁸ The diffraction grating can be changed but it requires a new alignment.

⁹ However the compressor length and the incidence angle are easily adjusted using translation and rotation plates respectively.

3. Numerical optimisation

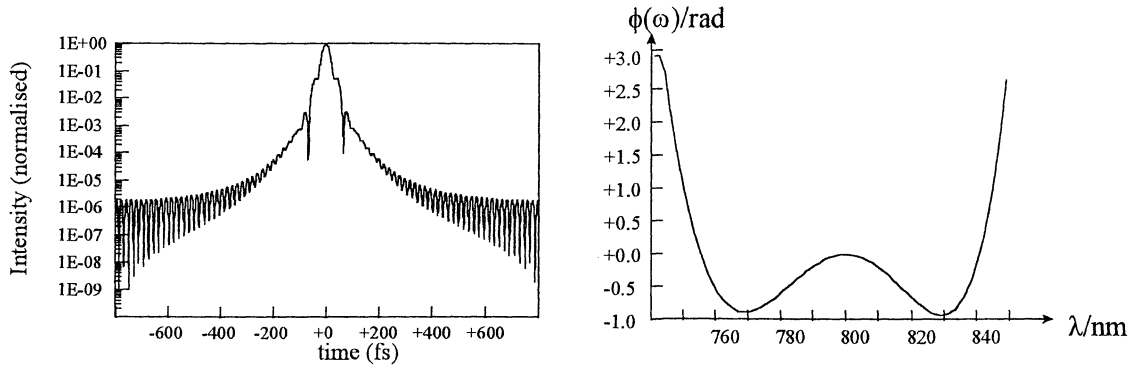


Fig 11. a. Calculation of temporal profile of the 25fs Gaussian pulse after passage through our optimised CPA chain. Notice the steps introduced by the spectral phase and the wings introduced by the spectral cut.
 b. Calculation of the spectral phase after passage through the optimised CPA chain. Notice that it has mainly the shape of a fourth order dispersion. The spectral phase components are calculated to : $\phi^{(2)} = -4.65 \cdot 10^2 \text{fs}^2$, $\phi^{(3)} = -2.06 \cdot 10^2 \text{fs}^3$, $\phi^{(4)} = 3.46 \cdot 10^5 \text{fs}^4$.

The parameters of the stretcher and the compressor were optimised with a ray tracing program developed at LOA. The simulation was made for a 25fs Gaussian pulse with a spectral range of 100nm, 752-852nm. The materials in the regenerative amplifier through which the laser beam passes are approximately: 520mm of Ti :sapphire (gain medium), 520mm of SiO₂ (polarizer) and 1000mm of KDP (Pockels cell). This corresponds to 28 cavity round-trips¹⁰. The incidence angle into the stretcher was chosen as 50° which corresponds to a diffraction angle of -11.18° for the central wavelength λ_0 , 801nm. The incidence angle into the compressor was chosen as 61,81° with a diffraction angle of 4.50°. This gives a difference in incidence angle of 11.81°. The compressor length was optimised to 504,8mm, which is 104.8mm longer than the stretcher length. These differences in incidence angle and length compensate for the spectral phase introduced by aberrations in the stretcher and dispersion due to materials in the regenerative amplifier.

The result of the numerical simulation is shown in the two graphs above. The 25fs pulse increases to 28.5fs after re-compression. The spectral phase is mainly a fourth order dispersion term, $\phi^{(4)}$, since the compressor and the stretcher only compensates for second and third order dispersion. The fourth order dispersion is caused by spherical aberration in the stretcher. Simulation without the regenerative amplifier gave a duration of 27.4fs and a spectral phase with 0.7rad peak to peak compared to 1rad with amplifier. This implies that fourth order dispersion is also introduced by the regenerative amplifier.

The calculated spectral phase is :

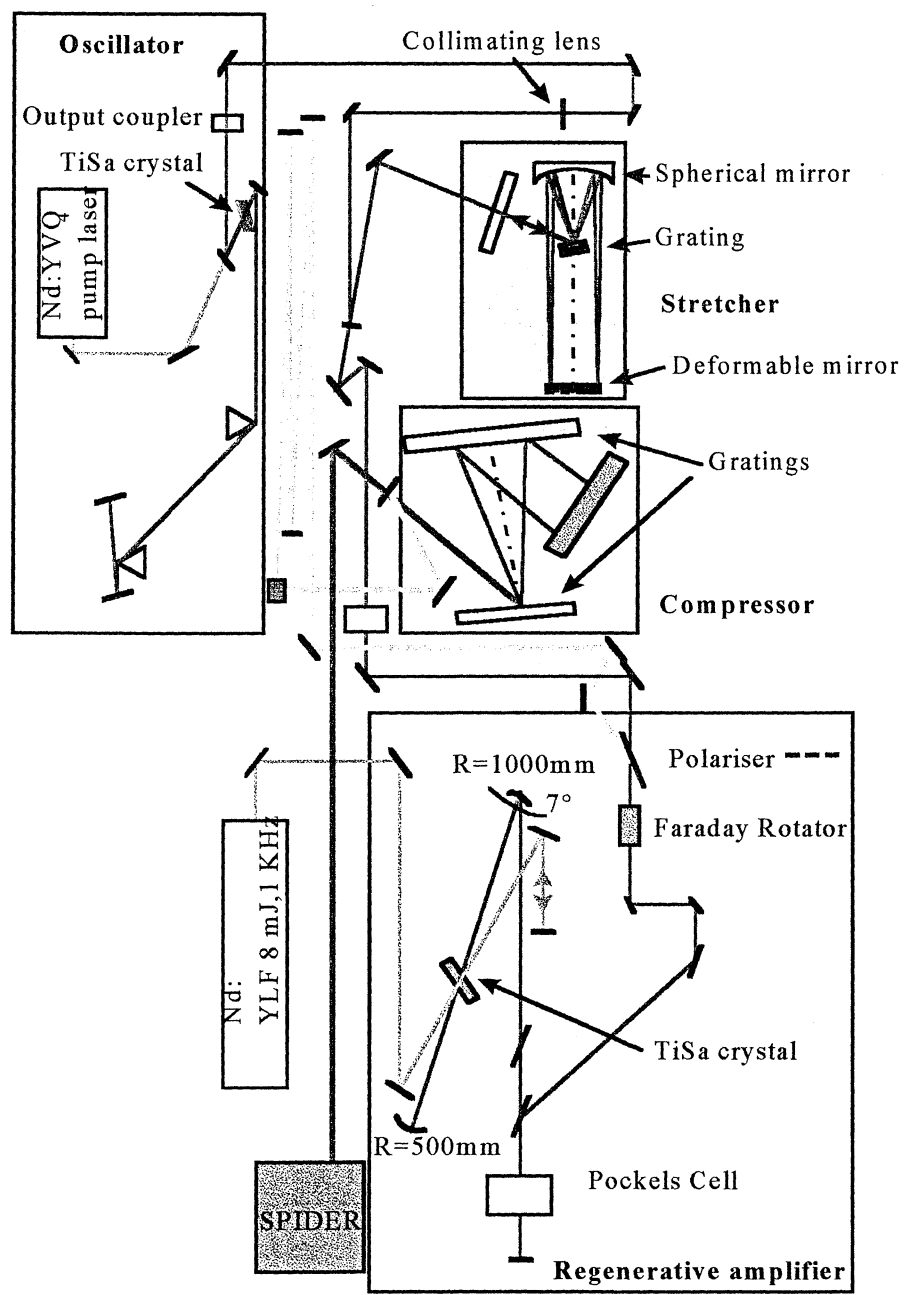
$$\begin{aligned}\phi^{(2)} &= -4.65 \cdot 10^2 \text{ fs}^2 \\ \phi^{(3)} &= -2.06 \cdot 10^2 \text{ fs}^3 \\ \phi^{(4)} &= 3.46 \cdot 10^5 \text{ fs}^4\end{aligned}$$

Notice that the positive fourth order dispersion, $\phi^{(4)}$, is compensated with a negative second order dispersion, $\phi^{(2)}$.

¹⁰ The number of round-trips have decreased to around 44 after optimisation of the regenerative amplifier.

4. Experimental set-up

4.1. Laser chain



Instruments

Pump Lasers :

Oscillator :

« Millenia V », Spectra Physics Lasers

Nd:YVO₄, cw, $\lambda=532\text{ nm}$, $P_{\text{max}}=5\text{ W}$

Regenerative Amplifier :

Q-switched and frequency doubled Nd :YLF, B.M.Industries

pulse duration : $0.75\mu\text{s}$, $\lambda=527\text{nm}$, $P_{\text{max}}=10\text{W}$

Pockels cell :

Pockels cell Timer&Driver, MEDOX

Digital delay and pulse generator :

model DG535, Stanford

Oscilloscope :

model 2465B, 400MHz, Tektronix

4.2. Oscillator

4.2.1. Technical information

The gain medium, Ti:sapphire crystal, is pumped longitudinally on-axis with a 3.2W continuous laser at 532nm. The output beam from the oscillator has a pulse energy of 2.6nJ and a repetition rate of approximately 100MHz. The bandwidth of the oscillator can be changed from 30nm to more than 100nm, however the cavity becomes more unstable the larger the bandwidth.

4.2.2. Pulse duration

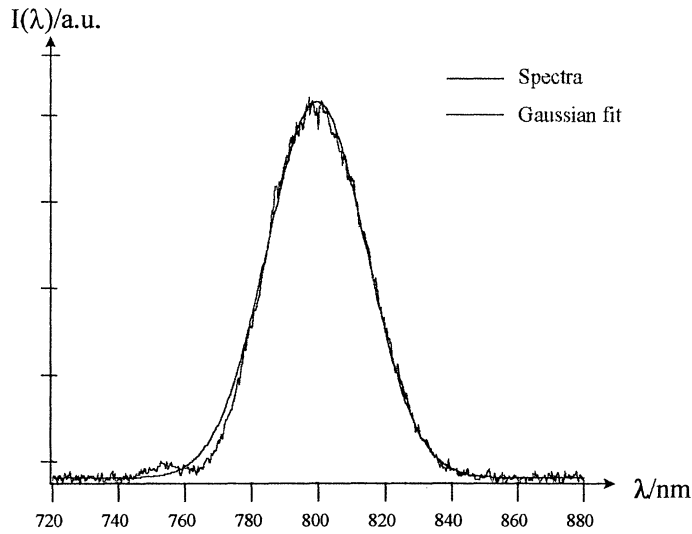


Fig 12. The spectrum of the output pulse from the oscillator and the corresponding Gaussian fit.

The spectrum of the output pulse from the oscillator is shown in the graph above. The Gaussian fit, was made in Femtplot, a calculation program developed at LOA. The curve is very close to Gaussian with a bandwidth of 35.2nm. The central wavelength is 799.4nm. The duration of the pulse was calculated with Fourier transform to 28.49fs. Calculation of the time-bandwidth product by development of equation (5) is as follows:

$$\Delta\tau \cdot \Delta\nu \geq K$$

$$\nu = \frac{c}{\lambda}$$

$$d\nu = \frac{c}{\lambda^2} d\lambda \Rightarrow \Delta\nu \approx \frac{c}{\lambda^2} \Delta\lambda$$

$$\Delta\tau \cdot \frac{c}{\lambda^2} \Delta\lambda \geq K \quad (6)$$

Insert the values from above :
 bandwidth : $\Delta\lambda = 35.2\text{nm}$
 duration : $\Delta\tau = 28.49\text{fs}$
 central wavelength : $\lambda = 799.4\text{nm}$

The time-bandwidth product is 0.471. This can be compared to the time-bandwidth product of a transform limited Gaussian curve which is $K=0.441$. The curve is close to being Gaussian, which is verified by the Gaussian fit, see fig. 12. This calculation was made in a program called Femto plot, for more information how the calculation was done see Appendix A.

4.3. Regenerative Amplifier

4.3.1. Set-up

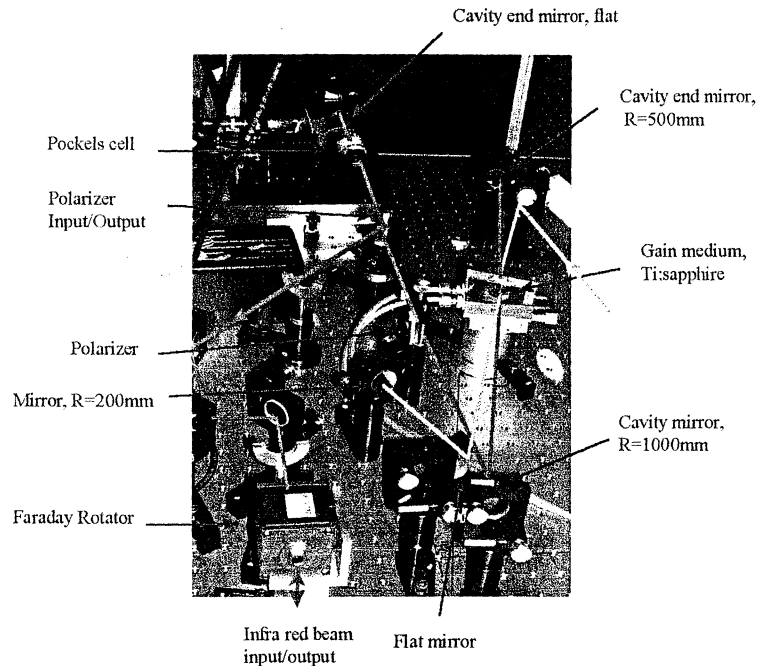


Fig 13. A photograph of the regenerative amplifier that was built during this thesis work. The regenerative cavity consists of three mirrors, two spherical and one flat, a Ti:sapphire crystal, a Pockels cell and two polarizers. The propagation path for the infra-red pulse is marked with red¹¹. The pump beam is focused in the Ti:sapphire with a lens, $f = 250\text{mm}$, outside the picture. The part of the pump beam that is transmitted through the crystal is retroreflected into the crystal with two mirrors, one flat and one concave, $R=200\text{mm}$. The Faraday Rotator does not turn the polarisation for the input beam, but turns the polarisation of the output beam with 90° . The path way of the input and output beam is then separated by a polarizer, not shown in the picture. The quality of the polarizer is important because amplified pulses that follows the input pulse path causes instability in the oscillator. These parasite pulses prevent the oscillator from remaining mode-locked.

The regenerative amplifier is a three mirror cavity. See three cavity mirrors in the fig 13. The gain medium is a Ti :sapphire crystal placed at Brewster angle to minimise losses. The crystal is pumped longitudinally, but off axis¹², with a Q-switched frequency doubled Nd :YLF laser. The frequency doubled Nd :YLF generates 8mJ pulses at 527nm.

4.3.2. Pockels cell

The Pockels cell contains a birefringent crystal, KDP. The orientation of the KDP's axis changes proportionally to the applied dc voltage. Hence by altering the voltage across the Pockels cell its polarisation property changes. For simplicity the Pockels cell and the polarizer are compared to a shutter that opens and closes, like in the theory section. The temporal behaviour of the Pockels cell is visualised in diagram 2. Notice that it is crucial that the shutter opens and closes faster than the time it takes the pulse to do a cycle in the cavity, $\sim 9\text{ns}$.

¹¹ In black and white format, this is the darker of the two paths marked.

¹² The gain medium is pumped slightly off axis, see figure, to avoid pumping through the end mirror of the cavity, which would otherwise be damaged.

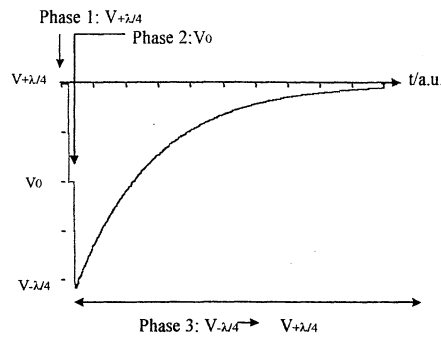


Fig 14: The voltage applied across the KDP crystal in the Pockels cell, as a function of time.

Phase 1: Closed shutter

The Pockels cell used is placed such that it functions as a positive quarter-wave plate¹³ when no voltage is applied across the KDP crystal.

Phase 2: Open shutter: Entrance

A voltage corresponding to a negative quarter-wave plate, a "negative quarter-wave voltage" is applied. Consequently the Pockels cell does not turn the polarisation of an incoming beam, since the positive and negative quarter-wave qualities cancel each other.

Phase 3: Closed shutter: Exit

To extract the amplified beam the tension is further decreased by another negative quarter-wave voltage. The Pockels cell becomes a negative quarter-wave plate. Finally the voltage across the Pockels cell is reset to zero.

4.3.3. Amplification process

The light beam from the stretcher is horizontally polarised and enters the cavity, by reflection on the polarizer. It is transmitted twice through the Pockels cell, which turns the polarisation 45 degrees each time, phase 1. The pulse is now vertically polarised and is transmitted through the polarizer. The Pockels cell property is changed, phase 2, no polarisation effect. The pulse is now trapped within the cavity, since passage through the Pockels cell does not change its polarisation. The pulse passes the gain medium twice per cavity round trip and increases in energy. This amplification process is visualised with a photodiode placed behind the end-mirror of the cavity and an oscilloscope, see diagram. When the pulse has reached its maximum energy the voltage across the KDP is again decreased. The Pockels cell returns to its original status of a quarter wave plate and turns the polarisation of the pulse 90 degrees. The amplified pulse is then reflected out of the cavity by the polarizer, phase 3.

¹³ A linearly polarised beam is turned 45 degrees to the right, looking in the direction of the propagating beam, after passage through the Pockels cell.

4.4. Compressor

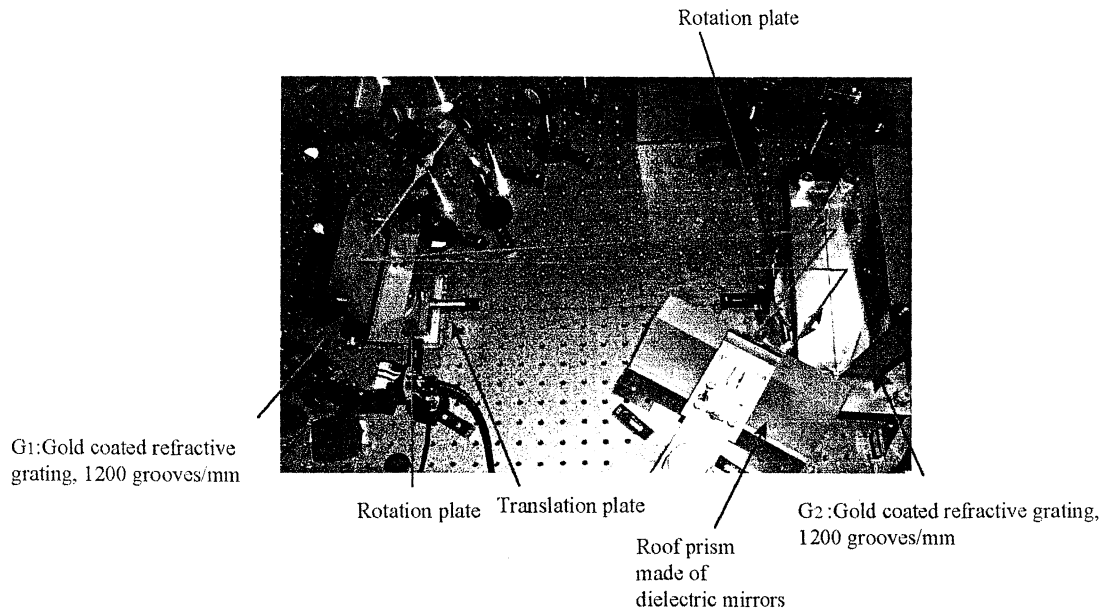


Fig 15. A photograph of the compressor installed during this thesis work. The incidence angle of the compressor is changed with the two rotation plates. It is very important that both gratings are turned the same angle so that they remain parallel, otherwise spatial chirp is introduced. Spatial chirp means that the pulse's wavelengths are distributed spatially. Spatial chirp is verified by looking at the shape of the beam spot. A spatially chirped pulse has a parabolic instead of a circular shape. The compressor length is adjusted with the translation plate.

The two gratings are gold coated and have a flatness of $\lambda/10$. The diffraction grating spacing is 1200grooves/mm. The first grating is placed on a translation plate so that the length of the compressor can be adjusted. Each of the two gratings is placed on two rotation plates. The first is a three-angle plate used when aligning the compressor. The second is used to adjust the incidence angle of the compressor and for alignment. It is very important that the two compressors remain parallel otherwise spatial chirp¹⁴ is introduced. The optimised compressor has an incidence angle of 59.50° and a length of 51.5 cm. The numerical optimisation, see the results chapter, gives 61.8° and 50.48 cm respectively.

¹⁴ Spatial chirp means that the beam spot is not homogenous, but the wavelengths are spatially separated.

4.5. Stretcher

The stretcher design is a variation, proposed by G. Cheriaux ref. [5], of the stretcher used in ref. [9]. The symmetry of the stretcher model in ref. [9] is exploited and one of the spherical mirrors in the telescope in ref. [9] is replaced with a plane mirror placed in the Fourier plane of the remaining spherical mirror. However in our set-up the plane mirror has been replaced with a deformable mirror, DM. The shape of the DM is chosen such that it introduces a spectral phase opposite to that of the output beam. The deformable mirror corrects therefore the spectral phase introduced during the pulse's propagation through the laser chain. This method relaxes the requirement of an aberration free stretcher design and saves alignment time for the user.

4.5.1. Stretcher model

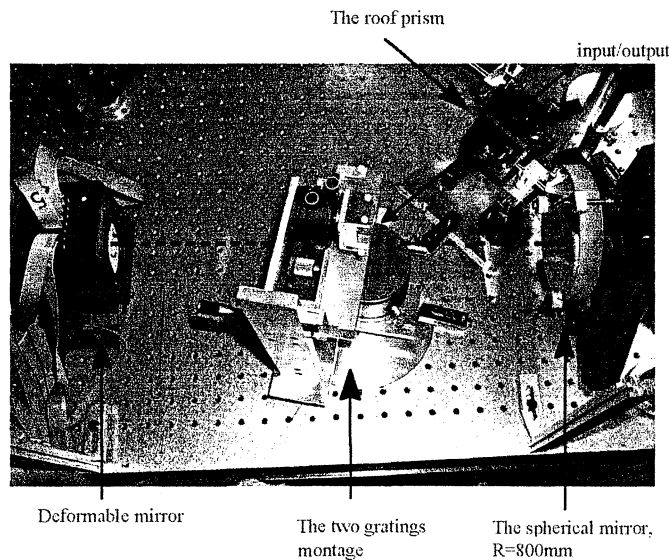


Fig 16. A photograph of the stretcher built during this thesis work. The optical axis is marked with a dashed line, for the detailed beam path see next figure. The alignment of the components is critical for the performance of the stretcher. The alignment procedure of this particular stretcher model is presented in Appendix A.

The two gratings are placed on top of each other separated by a gap of 34 mm. The diffraction gratings are gold coated with a flatness of $\lambda/10$ and have 1200 grooves/mm. The small grating, on top, is 30 mm long, and the bottom grating 160 mm long. The diameter of the concave mirror is 100 mm and its flatness λ . The Xinetics deformable mirror has a diameter of 50 mm with a flatness of $\lambda/20$ ²¹.

²¹ This is the original flatness of the mirror before the actuators are glued to its reversed side.

Top view of the stretcher :

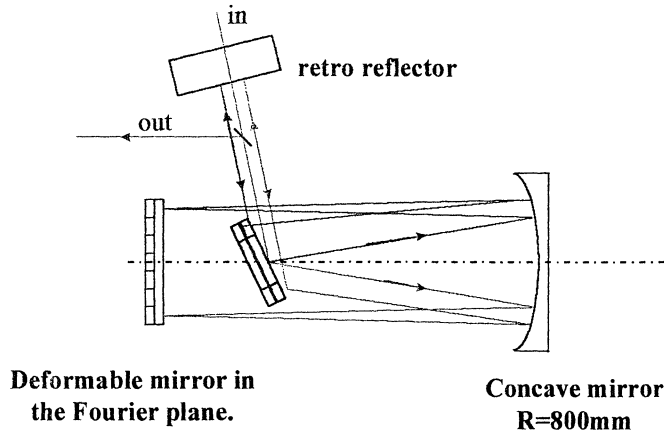


Fig 17. The ray trace in the stretcher, top view.

The pulse is incident on the top grating, above the optical axis, and diffracted at order -1. The refracted beam is then reflected by the spherical mirror and focused on the deformable mirror. The spherical mirror then reflects the beam again, this time below the optical axis, and incident on the lower grating. The beam is refracted again and exits parallel. The roof prisms return the beam for double passage in the stretcher at a distance closer to the optic axis.

4.5.2. Grating frame

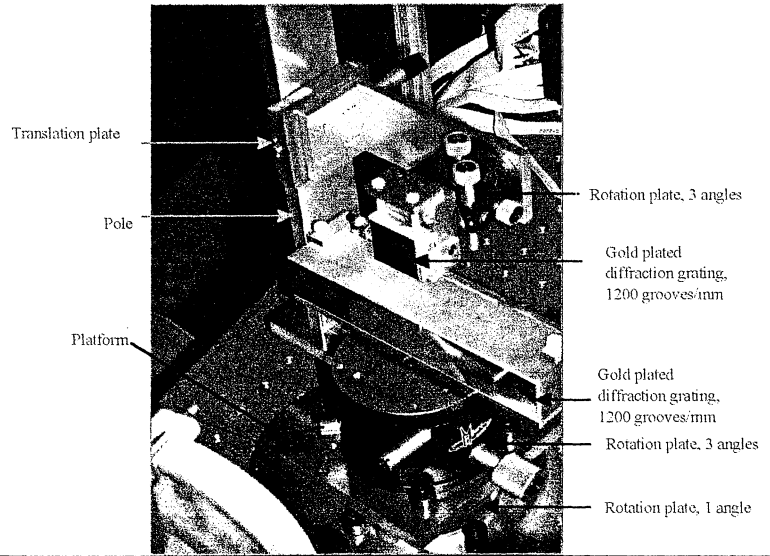


Fig 18. A photograph of the grating frame.

The design of the grating frame had several requirements to fulfil. First, there has to be a gap between the two gratings, otherwise the beam cannot pass. This is solved by placing the smaller grating at the end of a lever, which is attached to a pole, see fig. 18. Secondly, it must be possible to align the two gratings independent of each other, which means that each grating must be placed on a control plate, adjustable in three angles. Thirdly, the horizontal distance between the two gratings must be controllable, so that the stretcher is symmetrical. Hence the lever arm is fixed at a translator plate so that the small grating can be moved horizontally. Lastly the two gratings must lie on the same rotation axis and it must be possible to rotate them together, to conserve the incidence angle. The pole and the lower grating are fixed to a

plate, which in turn is attached to a rotator plate. The centre of the two gratings is placed on the rotation axis of the rotator plate.

Side view of the stretcher :

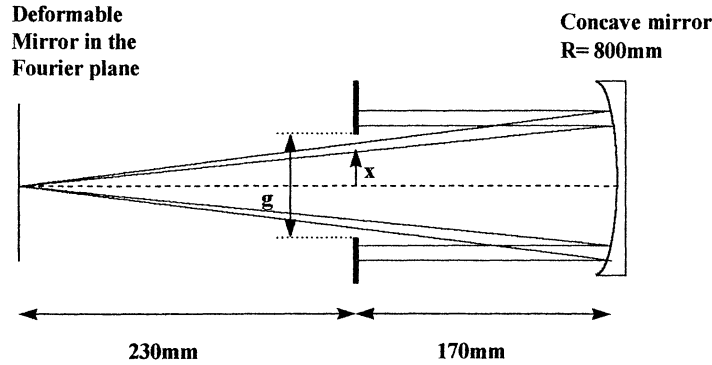


Fig 18. The ray trace in the stretcher, side view. The gap between the two gratings is marked with g. The distance between the light ray and the optic axis at the position of the gratings is marked with x.

The pulse should be vertically placed as close to the optic axis as possible, in order to avoid aberrations. The lower gap limit is set by the diameter of the laser pulse and the criteria of double passage. Each grating must have space for two beam spots separated vertically by a distance of 5 mm. This distance is set assuming the spot diameter to be 3 mm. Further the lower beam spot has to be 2 mm from the edge of the grating since the first millimetre of the grating cannot be used. Hence the highest beam spot has to be at least 9 mm from the edge of the grating. The minimum input height for which the light rays passes between the gratings is calculated using the law of Thales :

$$\frac{y}{400} = \frac{y-9}{230} \Rightarrow y = 21mm \quad (7)$$

The entrance height, y, was chosen to 25 mm and the distance between the gratings, g, was set to 34 mm, see fig. 18.

4.5.3. Feedback loop

The shape of the deformable mirror is set with a feedback loop. The feedback loop consists of an instrument that measures the spectral phase called the SPIDER, the deformable mirror and an algorithm written in Labview. The two latter¹⁶ parts are explained in the paragraphs below.

¹⁶ The SPIDER is explained in the last section of this chapter.

4.5.3.1. Deformable mirror

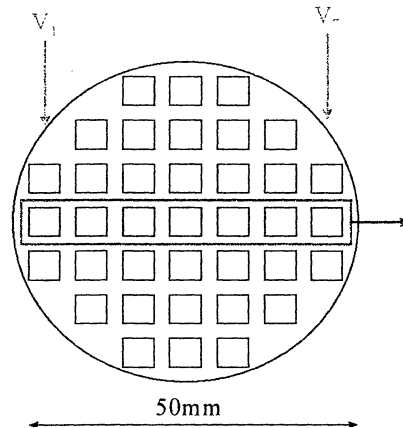


Fig 19. A sketch of the deformable mirror, with its 37 actuators marked as squares.

The shape of the deformable mirror is set by applying voltage across piezo plates attached on its reverse side. The thirty-seven actuators are glued in horizontal lines on the reverse side of the plane mirror, seven along the line of our interest. The actuators change length when voltage is applied across them and deform the surface of the mirror. To avoid unnecessary stress in the mirror the same voltage is applied along each column. The voltage range is 90 V, and the function between voltage and displacement d is quadratic²³. The maximum displacement is 10 μm with a minimum step of 40 nm, $\lambda/20$. The flatness of the mirror was $\lambda/20$ before the piezo plates were glued on to it. When the piezo plates are glued onto the mirror they introduce stresses in the mirror. This effect is observable because it causes periodic bumps on the spectral phase.

4.5.3.2. Control algorithm

The deformable mirror is placed in the Fourier plane of the spherical mirror. The frequency components of the pulse spectrum are hence aligned. Therefore, the actuators acts on different parts of the pulse's spectrum. The actuators on the edges of the mirror have less impact on the spectral phase than the central ones due to the construction of the mirror. These are therefore programmed to follow their respective neighbour.

First the spectral range of each actuator is calibrated so that the mirror's diameter correspond to the spectral phase measured by the SPIDER. Then a voltage is applied to only one actuator and a bump on the spectral phase is created. The wavelength at which the bump occurs is the central wavelength of that actuator's spectral range. When all zones have been set, the tension is set to 10V to reset the spectral phase. A reference phase, the flat phase, is set to the phase of the central wavelength. Calibration is finished and the feedback loop is initialised.

²³ $f(d)=kV^2$

4.5.3.3. Feedback loop

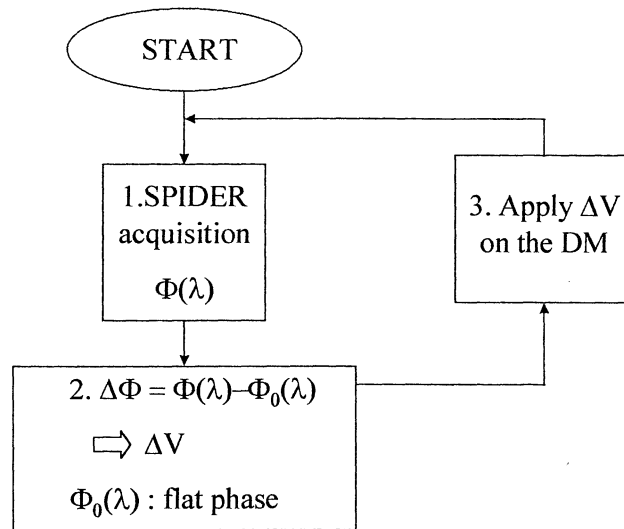


Fig 20. The feedback loop.

1. The SPIDER calculates the spectral phase $\phi(\lambda)$.
2.
 - a. The average spectral phase, for example ten measurements, is calculated.
 - b. The reference phase is then subtracted from each of the actuators' spectral phase components.
 - c. The corresponding voltage difference is calculated.
3. The calculated voltage is applied across the corresponding actuator on the deformable mirror.

4.5.3.3. Capacity of the deformable mirror

The performance of the deformable mirror and the feedback loop had been tested in a zero dispersion line before being implemented in the stretcher. The dynamic range of the mirror was more than 20 rad. This is far more than needed in our CPA system. A flatness of the spectral phase better than 0.4 radians on a 70nm spectral range was achieved. The deformable mirror corrected non-linear phase up to the 5th order of dispersion.

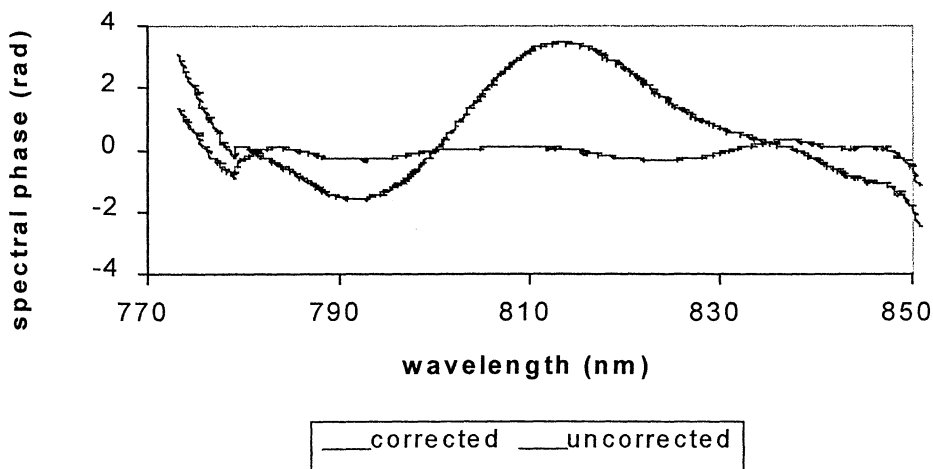


Fig 21. The spectral phase before and after correction when the deformable mirror was placed in a zero dispersion line.

4.6. SPIDER

The spectral phase and the duration of the output pulse were measured with the SPIDER technique developed by C. Iaconis et al in 1998, ref. [10]. SPIDER is the abbreviation of Spectral Phase Interferometry for Direct Electric field Reconstruction. The electric field of the input pulse is reconstructed with measurements from spectral shearing interferometry and algorithm calculations. In the following section an introduction to the SPIDER is presented, for more information see ref. [10,11].

4.6.1. Spectral shearing interferometry

The spectral phase and the time dependent intensity of the laser pulse is measured with spectral shearing interferometry. The information obtained is then used to reconstruct the electric field of the input pulse. The basic spectral shearing interferometer consists of two linear filters, two beam splitters and a spectrometer, see figure below.

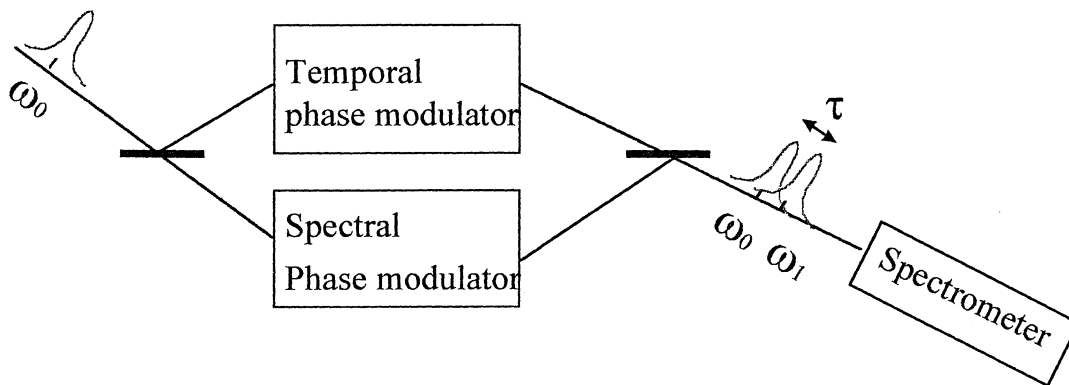


Fig 22. One pulse with central frequency ω_0 is divided into two replicas by the beamsplitter. One of the pulses passes through the temporal phase modulator and is frequency shifted. Its new central frequency is $\omega_1 = \omega_0 + \Omega$. The other pulse passes through the spectral phase modulator and is delayed a time τ . The two pulses are reunited after the second beamsplitter. The sum frequency mix of the two pulses is then measured with the spectrometer.

The input pulse is divided into two identical parts by the first beamsplitter. One pulse passes through the linear temporal phase modulator and is shifted in frequency with Ω . The second passes through the linear spectral phase modulator and is delayed a time τ . The two pulses are then recombined by the second beamsplitter. The sum frequency mix of the two pulses is measured with the spectrometer. The measured result is a spectrum with fringes, which are caused by the delay t between the two pulses.

The spectral phase of the input pulse causes differences in the nominal spacing of the fringes. To be able to measure this difference the spectral resolution has to be sufficient. The spectral interferometer is limited to measure picosecond pulses²⁴, ref. [11], if the temporal phase modulator is not used. The frequency shift between the two pulses increases the space in-between the fringes. The resolution of the spectral phase is improved. The temporal phase modulator is therefore necessary in order to measure the spectral phase for femto second pulses.

²⁴ This is the resolution limit of the spectrometer.

4.6.2. SPIDER set-up

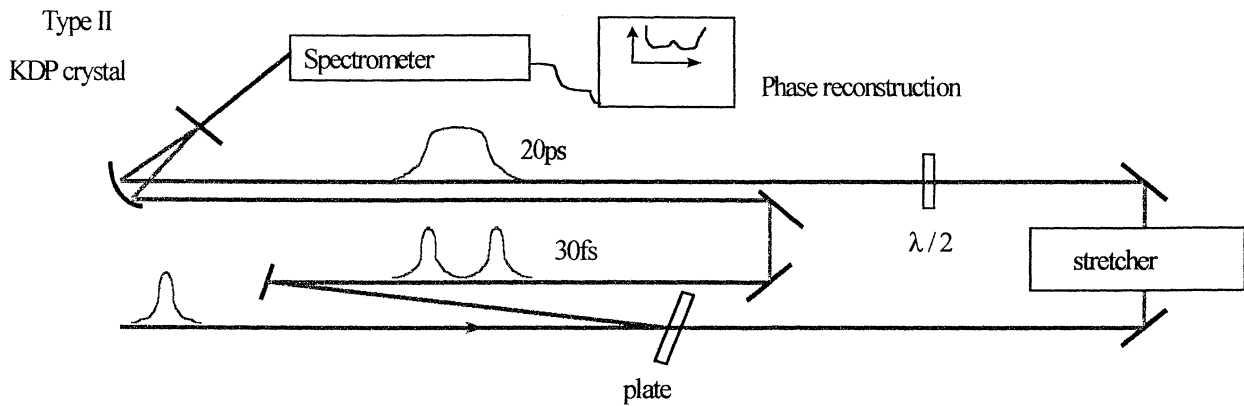


Fig 23. The output pulse from the laser chain is incident on the glass plate. Two replicas are reflected at each interface. The two replicas are separated by a time τ . However the majority of the pulse is transmitted and stretched in the stretcher. After the stretcher the pulse is incident on a half-wave plate, which turns its polarisation 180°. The two replicas and the stretched pulse, which are perpendicularly polarised with respect to each other, are rejoined in the non-linear crystal, KDP type II. The result is two frequency-sheared pulses whose sum frequency mix is resolved by the spectrometer. The result is then used to reconstruct the spectral phase of the laser chain's output pulse.

The input pulse is incident on a glass plate, which is 150 μm thick. Parts of the pulse are reflected at each of the two interfaces of the plate. The two reflected pulses are replicas of the original pulse and are separated by a time τ . *The plate is the linear spectral phase modulator.* The majority of the pulse is transmitted. The transmitted pulse is then stretched linearly in time in a stretcher. The stretched pulse then passes a half-wave plate²⁵, which turns its polarisation 180°. The two horizontally polarised replicas are interfered with the vertically polarised chirped pulse in a non-linear crystal, Type II KDP crystal. The result is two frequency-doubled pulses. The pulses are frequency sheared, since they have interacted with different parts of the chirped pulse's spectrum. *The stretcher and the non-linear crystal together behave as a linear temporal phase modulator.* The sum frequency mix of the two pulses is then analysed with a spectrometer and the spectral phase reconstructed.

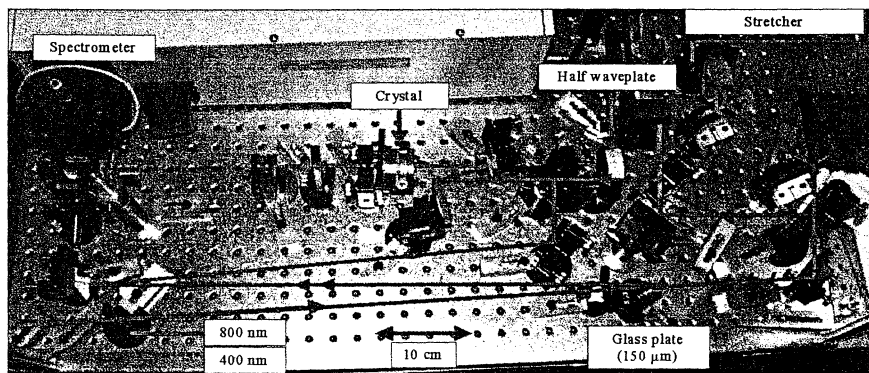


Fig 24. The SPIDER used during the experiment.

²⁵ The half-wave plate is necessary because frequency doubling is created in a type II crystal, which requires perpendicular polarised waves.

5. Results

The object with this master thesis was to improve the spectral phase of the output pulse from a chirped pulse amplification system using a deformable mirror in the stretcher. At the start of this project only the oscillator existed. The main time of this master thesis has hence been to build and optimise the other three components in the laser chain: the stretcher, the compressor and the regenerative amplifier. The stretcher and the compressor designs have been described in section 4.5 and 4.4 respectively. In this section the following results are presented: first, the performance of the regenerative amplifier²⁶, second, that of the deformable mirror in the feedback loop.

5.1. Regenerative Amplifier

5.1.2. Objective

The aim was to build a regenerative amplifier that amplifies the energy of the input pulse to about 1mJ. The output pulse should have the largest bandwidth possible, prefer over 30 nm since the bandwidth limits the duration of the pulse after re-compression. Further the number of round-trips in the cavity should be minimised in order to reduce dispersion introduced in the cavity. The output beam's mode has to be TEM₀₀ in order to propagate well through the laser chain.

5.2.2. Results

5.2.3. Free-running mode

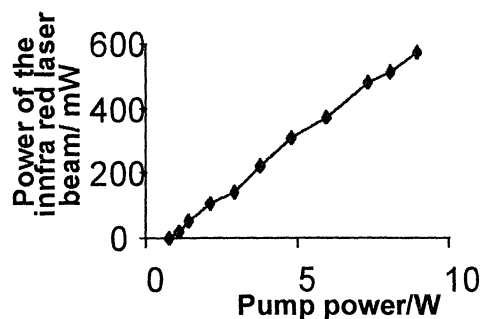


Fig 25. The relationship between pump power and the laser beam in the regenerative when the cavity was in free-running mode. These measures were taken before the Pockels cell was installed into the cavity. The pump laser works at 1kHz and the infra-red beam is the reflection from the polarizer.

First the cavity was optimised in free running mode²⁷. The result is shown in fig. 25. It shows the nearly linear relationship between pump power and laser power. Further the threshold had been minimised and corresponds to 1.0W in pump power.

²⁶ The design of the regenerative amplifier is presented in section 4.3.

²⁷ Free running mode is when the regenerative operates without any injection.

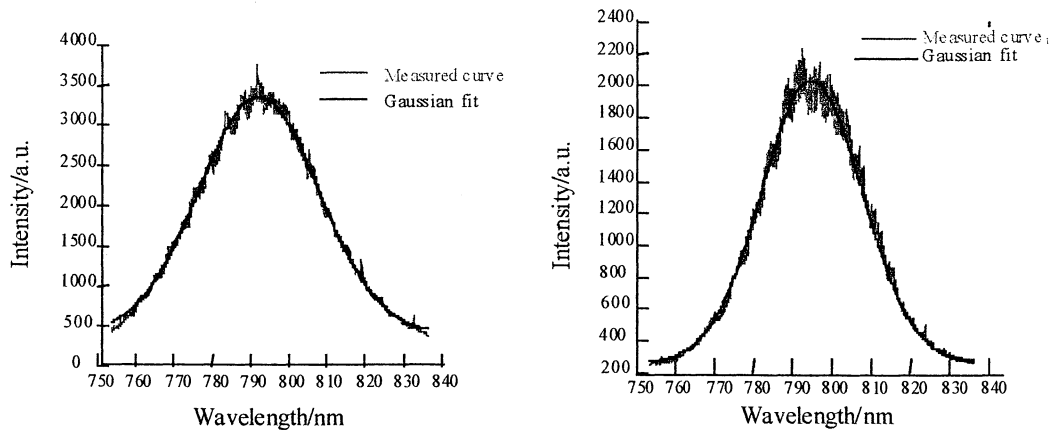


Fig 26. a. The spectrum of the laser beam created at free-running mode. It is close to Gaussian and the FWHM is 36.7nm.
 b. The spectrum of the amplified pulse. The pulse's has passed 16 round-trips in the cavity and increased in energy from 50 μ J to 0.7mJ.
 The FWHM has decreased from 35.2nm to 30.2nm due to gain narrowing.

The spectra of the pulses when the regenerative is in free-running mode, a, and with injection, b, are shown in the figure above. The FWHM are 36.7 nm and 30.2 nm respectively. Both curves are close to Gaussian, see fig. 26. The FWHM is smaller when a pulse is injected because the pulse exhibited a greater effect of gain narrowing. The pulse had a FWHM equal to 35.2nm before entering the regenerative amplifier²⁸.

5.2.4. Amplification

The energy of the output beam is 0.7mJ and the number of round-trips 22. The low energy level is partly due to thermal effects in the gain medium. The thermal effects change the refractive index of the Ti:sapphire as a function of temperature. An undesirable convergent lens is hence introduced into the cavity, which reduces the performance of the cavity. We tried to remove this effect by increasing the pump beam diameter in the gain medium. Unfortunately the cavity losses were larger than expected and the output energy did not increase. Further a second polarizer was added within the cavity to remove a birefringence effect. This effect was caused by the difference in polarisation axis of the Ti:sapphire crystal and the KDP crystal in the Pockels cell. The birefringence effect was noticed during calibration of the SPIDER because it caused a spectral modulation, which made it impossible to determine the nominal spacing in-between the fringes.

5.3. Deformable mirror

5.3.1. Objective

The aim was to correct the residual spectral phase introduced in a CPA system with a deformable mirror. The higher order dispersion terms decrease the contrast and increase the pulse duration. Usually the spectral phase is corrected for in an added zero dispersion line, ref. [3]. To avoid the added losses our deformable mirror was placed in the Fourier plane of the stretcher. The diameter of the mirror is 50 mm, which corresponds to 100 nm in bandwidth.

²⁸ These values were taken when the synchronisation between the pump beam and the input beam was controlled with signals from the oscillator. The bandwidth of the output pulse from the oscillator had therefore to be small so that the oscillator was stable.

5.3.3. Results

5.3.3.1 Spectral phase

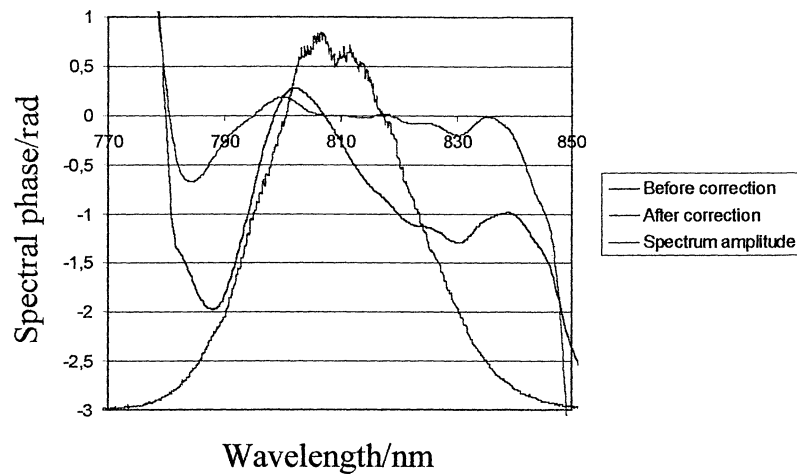


Fig 27. The spectrum of the laser pulse measured with the SPIDER.
The two other curves are the spectral phases before and after correction by the deformable mirror.
The flatness of the spectral phase is improved from 2 rd peak to valley to 0.4 rd over a 45nm range

The graph above shows the spectral phase of the re-compressed pulse before and after correction with the deformable mirror. The deformable mirror corrects well for the centre wavelengths, which correspond to the centre of the mirror. Since the mirror is placed in the Fourier plane this corresponds to the centre of the mirror. Hence the actuators on the border of the mirror have less effect on the spectral phase. There are two explanations to this effect. The first is a measurement problem. The SPIDER has difficulty to distinguish the fringes from noise at the edges of the spectrum, see the sharp change in phase at $\lambda = 780$ nm and $\lambda = 840$ nm. The second explanation is a construction problem, which shows the limit of the performance of the mirror used. The number of actuators per column is only three at the edges of the mirror, but seven in its centre. Would a rectangular mirror with equal number of actuators in each line perform better than the circular mirror used?

The spectral phase was improved from 2 rad to 0.4 rad peak-to-valley on a 45 nm spectral range. This corresponds to $\lambda/16$, which is the limit of the deformable mirror. The deformable mirror had a flatness of $\lambda/20$ before the actuators were glued on its reverse side. However the actuators decrease the flatness because they introduce constrain in the mirror. The effect of the actuators on the flatness is visible as small periodic bumps. This is a construction problem, which shows the limit of this deformable mirror.

Notice also the difference between the uncorrected spectral phase and the spectral phase calculated with the ray-tracing program. The ray-tracing program considers all optical material perfect. In practice the optical components have defaults and are sources of aberrations. The aberrations cause defaults in the spectral phase, which was not taken into account in the numerical optimisation. Further the compressor had not been perfectly optimised in order to show the potential of the feedback loop and especially the deformable mirror.

Finally an important feature of the feedback loop is that it saves time for the user. It took less than 15 minutes to correct the spectral phase, a time that should be decreased with an

optimised algorithm. However the feedback loop is still faster and less tedious than optimisation of the incidence angle and the compressor length.

5.3.3.2. Contrast and duration

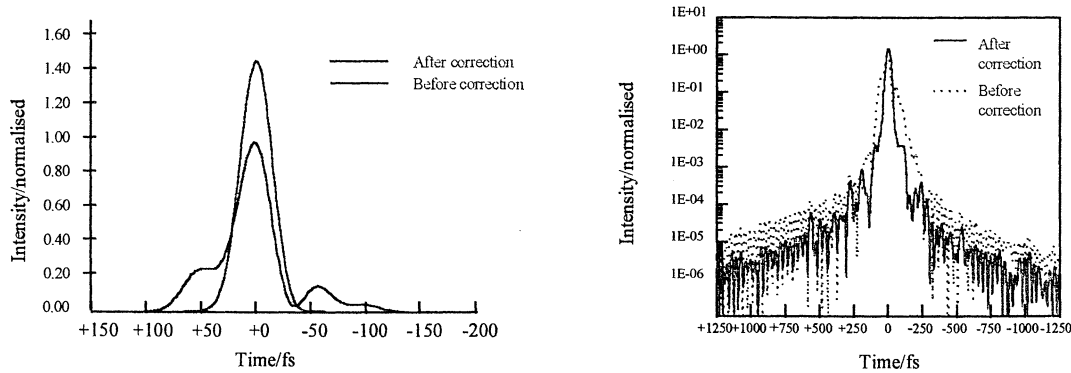


Fig 28. a. The temporal profile of the output pulse before and after correction with the deformable mirror. The pulse is more symmetric after correction and the pre and post implosions are almost eliminated.
b. The temporal profile of the output pulse in logarithmic representation.

The improvement of the spectral phase has a distinct effect on the temporal pulse shape, see the two graphs above. The pulse becomes more symmetrical, see fig 28a, after correction. The energy lost in the pulse's wings becomes concentrated in the central peak. The peak intensity increases approximately by a factor of 1.5 at $t=0$, see fig 28a.

The logarithmic representation gives more detailed information and shows the temporal profile on a ten times larger time scale. The concentration of energy in the central pulse peak increases considerably after correction, see fig. 28b. Further the pulse's wings are lower. The remaining spectral phase after correction causes a symmetrical pedestal at $t = \pm 100$ fs, corresponding to $I \approx 10^{-2}$ on the normalised scale. The pedestal should be eliminated if the spectral phase is made flatter over a larger spectral range. However, the wings starting at $t = \pm 250$ fs and $I \approx 10^{-4}$ are caused by the spectral cut in the stretcher. This is an effect of the finite size of the deformable mirror and cannot be reduced without changing mirror.

The duration of the laser pulse decreased from 37 fs to 35 fs when the spectral phase was reduced. These values were calculated in Femtplot with a precision of 1.6 fs. The decrease in duration was expected since the shape of the pulse becomes closer to Gaussian when the spectral phase is reduced.

6. Conclusion and Prospects

The first attempt to correct the residual spectral phase with a deformable mirror placed in the stretcher of a 35 fs, 1 kHz laser was carried out at Laboratoire d'Optique Appliquée, ENSTA - Ecole Polytechnique-CNRS, Paris. This experiment required a special stretcher design which, together with the compressor and the regenerative amplifier, were built during the project.

The spectral phase was reduced by using a feedback loop including a SPIDER, an algorithm and a deformable mirror. The SPIDER calculated the spectral phase with a precision of at least 0.1 rd. The calculated spectral phase was then the input parameter in the algorithm. The algorithm calculated the new shape of the DM. The deformable mirror was placed in the Fourier plane of the stretcher and acted therefore independently on the different spectral components.

The result obtained was an improvement of the flatness of the spectral phase from 2 rad to 0.4 rad peak-to-valley on a 45 nm spectral range. This corresponds to a flatness of $\lambda/16$, which was the limit of the DM's capacity. The improved flatness resulted in a distinct increase of the pulse's temporal contrast.

The future aspect is to improve the flatness of the spectral phase, increase the spectral range and improve the algorithm. The spectral phase can be reduced by replacing the deformable mirror with a mirror that has more pixels²⁹ and a greater flatness. The spectral range was primarily limited by the SPIDER because it had difficulty distinguishing the spectral phase³⁰ from noise at the edges of the spectrum. Hence to increase the spectral range the bandwidth of the laser pulse has to be increased. The bandwidth is limited due to gain narrowing in the regenerative amplifier. To avoid gain narrowing and increase the spectral width, a filter can be placed before the entrance or in the regenerative amplifier. The filter absorbs a band of wavelengths and introduces therefore losses in the pulse's spectrum at these wavelengths. A larger spectral range will be amplified in the regenerative amplifier if a filter is chosen that absorbs the central wavelengths of the laser pulse, around 800nm, because gain narrowing will be eliminated.

Finally, a new alternative to correct the residual phase in a CPA system has been demonstrated. The method improves the pulse contrast and saves alignment time for the user. However this is just a first step and the spectral phase can still be improved with a more precise deformable mirror and a larger measurable spectral range.

²⁹ The deformable mirror used has seven actuators in the line of interest.

³⁰ The spectral phase is measured as the difference from the nominal fringe spacing in the SPIDER spectrum. These fringes are the result of a sum frequency mix of two spectrally sheared pulses, hence there are less fringes at the edges of the spectrum.

Acknowledgements

First, I would like to acknowledge my supervisor at Laboratoire d'Optique Appliquée, Dr. Gilles Chériaux, for his confidence and encouragement during this thesis work. Especially for the independence in the laboratory, which gave me a chance to learn by practice, which was a great joy!

Further I would like to thank:

- Mr. Jean-Paul Chambaret and everyone in the ELF group at LOA, ENSTA-Ecole Polytechnique. Thanks for your professional guidance and for making me feel like a member of your team.
- My supervisor Prof. Anne L'Huillier at the Division of Atomic Physics at Lund's Institute of Technology, LTH, Sweden. For giving me the opportunity to make my thesis work at LOA and for your support.
- Kim Ta Phuoc for always taking your time to discuss and solve problems whether it concerned laser physics or culture differences.
- Jesper Marklund for correcting my English.

References

1. C. Le Blanc, "*Principes et Réalisation d'une Source Laser Terawatt Femtoseconde Basée sur le Saphir Dope au Titane. Caractérisation des Impulsions Produites et Démonstration du Régime d'Intensité au Niveau de $10^{18}W/cm^2$* ", Doctor thesis, Ecole Polytechnique(1995)
2. G.Chériaux, P. Rousseau, F.Sahlin, J-P. Chambaret, B.Walker, L.F. Dimauro, "*Aberration-free stretcher design for ultrashort-pulse amplification* ", Opt. Lett., **21**, No. 6, March 1996
3. P. Tournois, "*Acousto-optic programmable dispersive filter for adaptive compensation of group delay time dispersion in laser system* ", Opt. Comm.,**140**, August 1997
4. C.Dorrer, F.Sahlin, "*Programmable phase control of femtosecond pulses by use of a non-pixelated spatial light modulator* ", Opt. Lett., **23**, 907, July 1998
5. G.Chériaux, "*Influences des distorsions de phase sur le profil d'impulsions femtoseconde dans l'amplification à dérive de fréquence. Application à la génération d'impulsions de 30 TW à 10 Hz dans le saphir dopé au titane.* " Doctor thesis, Université de Paris-Sud U.F.R. Scientifique d'Orsay (1997)
6. O.Svelto, "*Principles of Lasers*", Fourth Ed., Plenum Press NY, USA (1998)
7. E.B.Treacy, "*Optical Pulse Compression With Diffraction Gratings* ", IEEE Journal of Quantum Electronics, **5**,No. 9, September 1969
8. O.E.Marinéz, "*3000 Times Grating Compressor with Positive Group Velocity Dispersion :Application to Fiber Compensation in 1.3-1.6 μ m Region* ", IEEE Journal of Quantum Electronics, **23**,No. 1,January 1987
9. J.V.Rudd, G.Korn, S.Kane, J.Squier, G.Mourou, P.Bado, "*Chirped-Pulse Amplification of 55-fs Pulses at a 1-kHz Repetition Rate in a Ti:Al₂O₃ Regenerative Amplifier*", Opt. Lett., **18**, No. 23 (2044), December 1993
10. C. Iaconis, I.A.Walmsley, "*Self-Referencing Spectral Interferometry for Measuring Ultrashort Optical Pulses* ", IEEE Journal of Quantum Electronics, **33**, No. 4, April 1999
11. C. Dorrer, "*Caractérisation et modulation d'impulsions laser femtoseconde* ", Doctor thesis, Ecole Polytechnique (1999)

For the interested reader I recommend:

C.Rullière, "Femtosecond Laser Pulses, Principles and Experiments", Springer, Germany (1998)

For a more general introduction to laser physics, ref. [6].

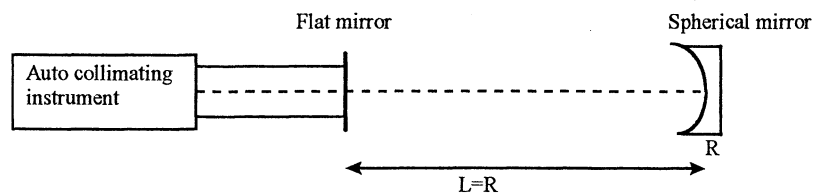
Appendix : Alignment of the stretcher

The alignment of the stretcher is critical for its performance. Aberrations have to be minimised and spatial chirp eliminated.

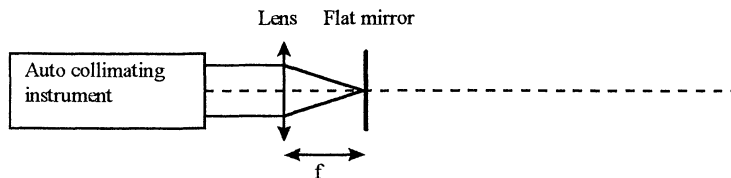
The stretcher was aligned with an auto-collimating instrument, A.I. The auto-collimating instrument contains a lamp and a hair cross. The lamp is the collimated light source and the fix hair cross the reference object of the instrument. The reflection, from the component to be aligned, is superposed onto the fix hair cross. When this occurs the two angles perpendicular to the propagation direction are conserved³¹. For practical reasons the hair cross is filmed with a camera and shown on a TV screen.

In this section the alignment procedure of the stretcher is presented. Before beginning the alignment, the auto-collimating instrument is adjusted such that the collimated output beam is parallel with the optic table.

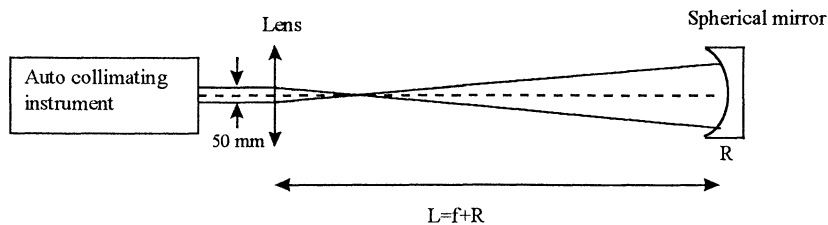
The spherical mirror



Step 1: A flat mirror is placed at a distance L in front of the spherical mirror. The distance L is equal to the curvature of the mirror. At this step the flat mirror is adjusted.



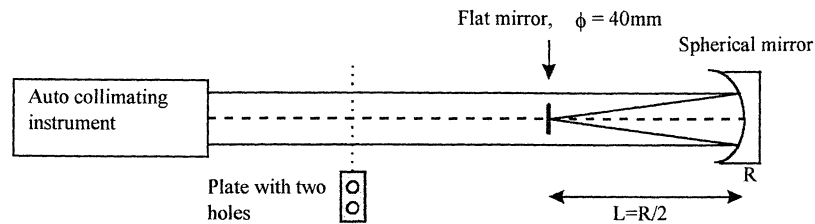
Step 2: A converging lens is placed at its focal distance from the plane mirror. In this step the lens and the distance f are adjusted.



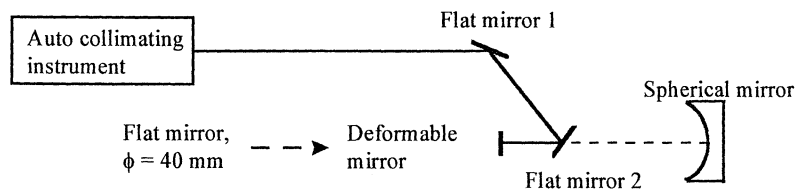
Step 3: The flat mirror is removed and the spherical mirror is aligned.

³¹ The angles, θ and φ , are the same for the output beam and the reflected beam.

The deformable mirror

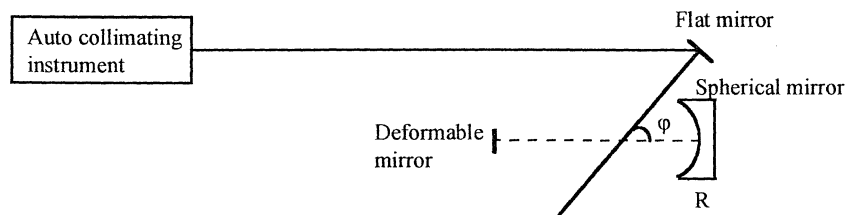


Step 1: A small flat mirror, diameter of 40mm, is placed at the spherical mirrors focal point, $f_M=R/2$. A plate with two holes is placed in the beam in order to avoid the reflex effect³², which prevents alignment of the flat mirror. The small flat mirror is aligned.



Step 2: The two flat mirrors, 1 and 2, are aligned while the small flat mirror is in the focal point of the spherical mirror. The small mirror is then replaced with the deformable mirror, which is aligned using the same configuration.

The incidence angle

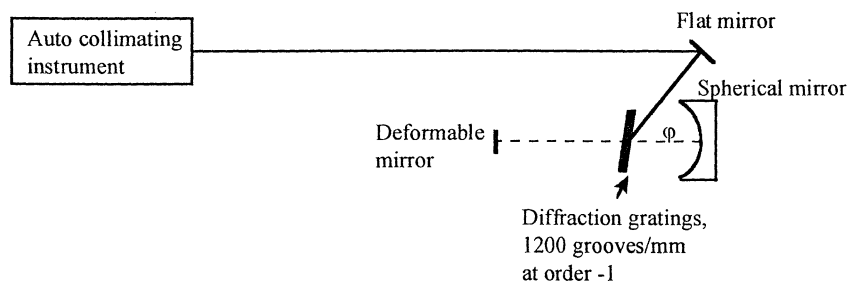


Where $\varphi = \theta_i + \theta_a$;

θ_i is the incidence angle and θ_a the diffracted angle for order -1 for the diffraction gratings.

The flat mirror is adjusted so that the light beam makes an angle φ to the optic axis of the stretcher.

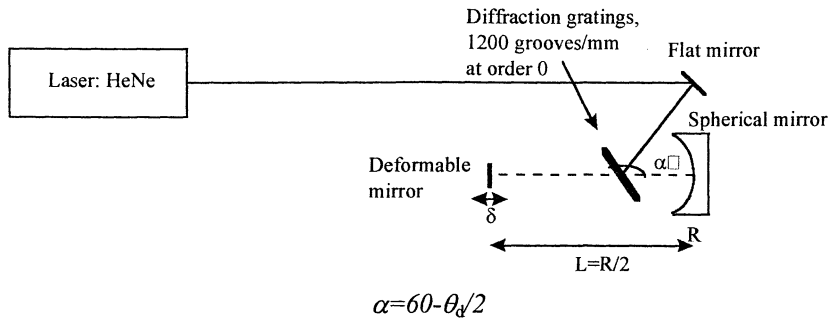
The gratings



Each grating is aligned independently using orders 1,0 and -1. Their surfaces are set parallel by superposition at order 0.

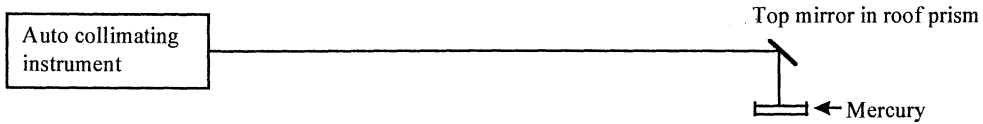
³² The flat mirror is placed in the focal point of the mirror and no matter how it is twisted the reflected beam from the spherical mirror to the A.I is the same. However by placing two holes in the light beam one verifies that the image of the two holes passes the two holes after reflection by the flat mirror.

Distance between the spherical mirror and the deformable mirror

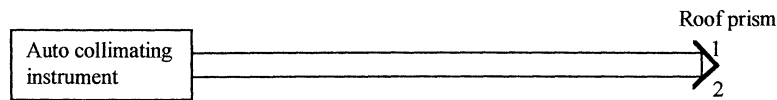


The grating frame is turned so that it makes an angle α with the optic axis. At this angle order 0 is along the optic axis, hence the two gratings function as mirrors. A He-Ne laser is used to precise the position, δ , of the deformable mirror so that it is at the focal point of the spherical mirror.

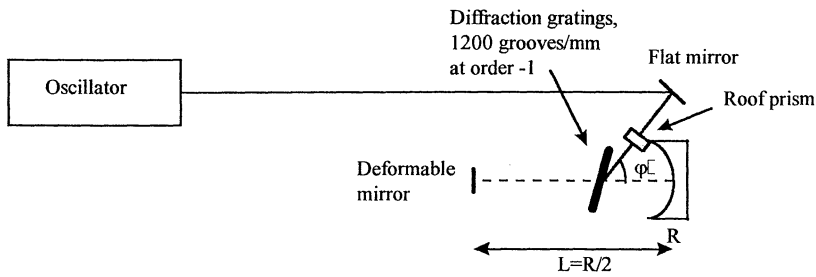
The roof prism



Step 1: The top mirror in the roof prism is aligned using Mercury as a mirror parallel to the optic table.



Step 2: The bottom mirror, number 2, is adjusted. The beam spot has to be incident on both mirror 1 and 2.



Step 3: The roof prism is positioned by using the oscillator. Use the infra red camera to verify that the two diffracted beams are in two vertical parallel lines on each grating and on the spherical mirror.